

# **Immunomodulation Using Micro-bead System for Chronic Wound Healing**

**Debadrita Paul**



Department of Biotechnology and Medical Engineering  
**National Institute of Technology, Rourkela**

# **Immunomodulation Using Micro-bead System for Chronic Wound Healing**

*Thesis submitted in partial fulfillment*

*of the requirements of the degree of*

***Master of Technology***

*in*

***Biotechnology***

*by*

***Debadrita Paul***

*(Roll Number: 215BM2010)*

*based on research carried out*

*under the supervision of*

***Prof. Devendra Verma***



May 2017

Department of Biotechnology and Medical Engineering  
**National Institute of Technology, Rourkela**



Department of Biotechnology and Medical Engineering  
**National Institute of Technology Rourkela**

---

May 25, 2017

## Certificate of Examination

Roll Number: *215BM2010*

Name: *Debadrita Paul*

Title of Thesis: *Immunomodulation Using Micro-bead System for Chronic Wound Healing*

We the below signed, after checking the thesis mentioned above and the official record book(s) of the student, hereby state our approval of the thesis submitted in partial fulfillment of the requirements for the degree of *Master of Technology in Biotechnology* at *National Institute of Technology Rourkela*. We are satisfied with the volume, quality, correctness and originality of the work.

---

Prof. Devendra Verma

Supervisor

---

Prof. Mukesh Kumar Gupta

Head of the Department



Department of Biotechnology and Medical Engineering  
**National Institute of Technology Rourkela**

---

**Prof. Devendra Vermar**  
Assistant Professor

May 25, 2017

## **Supervisors' Certificate**

This is to certify that the work presented in the thesis entitled *Immunomodulation Using Micro-bead System for Chronic Wound Healing*, submitted by *Debadrita Paul*, Roll Number *215BM2010*, is a record of original research carried out by her under my supervision and guidance in partial fulfillment of the requirements for the degree of *Master of Technology* in Biotechnology at *Department of Biotechnology and Medical Engineering of National Institute of Technology Rourkela*. Neither this thesis nor any part of it has been submitted earlier for any degree or diploma to any institute or university in India or abroad.

---

Prof. D. Verma  
Assistant Professor

# Dedication

*To my beloved family and friends...*

# Declaration of Originality

I, *Debadrita Paul*, Roll Number *215BM2010* hereby declare that this thesis entitled *Immunomodulation Using Micro-bead System for Chronic Wound Healing* presents my original work carried out as an M.Tech student of NIT Rourkela and, to the best of my knowledge, contains no material previously published or written by another Person, nor any material presented by me for the award of any degree or diploma of NIT Rourkela or any other institution. Any contribution made to this research by others, with whom I have worked at NIT Rourkela or elsewhere, is explicitly acknowledged in the thesis. Works of other authors cited in this dissertation have been duly acknowledged under the section "References". I have also submitted my original research records to the scrutiny committee for evaluation of my thesis.

I am fully aware that in the case of any non-compliance detected in future, the Senate of NIT Rourkela may withdraw the degree awarded to me on the basis of the present thesis.

May 25, 2017

NIT Rourkela

*Debadrita Paul*

# Acknowledgement

I would like to take this opportunity to express my sincere thanks to all those who have supported me in this endeavour.

I would like to begin by expressing my gratitude, indebtedness and respect to my guide **Prof. Devendra Verma**, without whose constant support, encouragement and guidance during the difficult times, this project would not have been possible. I would also like to thank Head of Department of Biotechnology and Medical Engineering, NIT Rourkela, **Prof. Mukesh Kumar Gupta** and all the **teachers of NIT Rourkela** for providing me with this opportunity and necessary facilities for the completion of my research work.

A special mention to **Prof. Indranil Banerjee** for their timely advices and suggestions; and also for their ardent intellectual Personality which translates as an inspiration towards Persuasion in young minds like that of mine. I am also obliged to **Prof. Mukesh Kumar Gupta**, **Prof. Bibhukalyan Prasad Nayak**, and **Prof. Sirsendu Sekhar Ray** for being helpful and providing me access to their lab.

I would like to convey my heartfelt gratitude to my friends, **Sourav Mishra**, **Jagrati Singh** and **Abhay Singh** and **Mr. Senthilguru Kulanthaivel**, for their help and advice throughout my project work.

Last but not the least, I would like to thank God and my parents who have been my pillar of strength at all times and the reason for who I am at this stage of my life.

May 25, 2017

NIT Rourkela

*Debadrita Paul*

# Abstract

Wound healing entails a series of complex stages where various cellular components of skin play a key role such as fibroblasts, keratinocytes, immune cells, endothelial cells, and extracellular matrix. The normal healing process can be divided into three distinctive phases: 1) inflammation, 2) proliferation and 3) maturation. Wounds which have failed to repair over a period of three months are characterized as a chronic wound. In India, high costs of treatment can persuade patients from seeking proper care, which leads to the development of complex and/or chronic wounds. There are several treatments being investigated, such as stem cell therapy, delivery of bioactive compounds (e.g., growth factors, cytokines, Peptides) to the wound site by encapsulating into microbeads. Macrophages play an important role in modulation of inflammatory response. Among two phenotypes of macrophage (e.g., M1 and M2), the M2 phenotype has a significant role in signalling of subsequent phases of wound healing. The aim of this project was the development of polysaccharide based microbeads, which would provide an anti-inflammatory environment to encapsulated macrophages. It was hypothesized that in presence of anti-inflammatory environment, un-activated macrophages may polarize to M2 phenotype and help in chronic wound healing by secreting anti-inflammatory cytokines and various growth factors in a sustainable and continuous manner. Pectin and polygalacturonic were chosen to develop macrophage encapsulated microbead system. Experimental results depicted that Pectin and PgA based microbeads could be used in this purpose since it was observed that these polymers are highly hemocompatible and do not have any cytotoxic effect on encapsulated cells. Encapsulated macrophages remained viable inside the beads for more than a week. Additionally, these beads promoted proliferation of macrophages. At the end morphological study showed that un-activated macrophages were polarized to M2 phenotype (macrophages attained an elongated structure) when seeded on Pectin and PgA based film. The polarization of un-activated macrophages to M2 phenotype in presence of anti-inflammatory environment inside the microbeads seems an effective strategy which might help further to treat chronic wounds within a shorter time span.

***Keywords: Macrophages; Wound healing; Chronic wound; M1 phenotype; M2 phenotype; Pro-inflammatory; Anti-inflammatory; Cytokines; Pectin; Polygalacturonic acid; Microbeads; Encapsulation***



# Contents

<b>Certificate of Examination</b> .....	<b>ii</b>
<b>Supervisors' Certificate</b> .....	<b>iii</b>
<b>Dedication</b> .....	<b>iv</b>
<b>Declaration of Originality</b> .....	<b>v</b>
<b>Acknowledgement</b> .....	<b>vi</b>
<b>Abstract</b> .....	<b>vii</b>
<b>List of Figures</b> .....	<b>xi</b>
<b>List of Tables</b> .....	<b>xiii</b>
<b>Introduction</b> .....	<b>1</b>
<b>1.1. Chronic Wound</b> .....	<b>1</b>
<b>1.2. Wound Healing</b> .....	<b>1</b>
<b>1.3. Factors Affecting Wound Healing</b> .....	<b>2</b>
<b>1.4. Objectives</b> .....	<b>4</b>
<b>Review of Literature</b> .....	<b>5</b>
2.1. Application of Stem Cells in Chronic Wound Healing.....	<b>5</b>
2.2. Application of Peptides in Chronic Wound Healing.....	<b>6</b>
2.3. Application of Peptides in Chronic Wound Healing.....	<b>6</b>
2.4. Application of Growth Factors in Chronic Wound Healing .....	<b>9</b>
2.5. Application of Cytokines in Chronic Wound Healing .....	<b>10</b>
2.6. Application of Macrophages in Chronic Wound Healing.....	<b>12</b>
2.7. Application of microencapsulation of cells in chronic wound healing .....	<b>14</b>
2.8. Rationale of current study .....	<b>15</b>
<b>Materials and Methods</b> .....	<b>16</b>
3.1. Materials.....	<b>16</b>
3.2. Fabrication of centrifuge tube-syringe setup.....	<b>16</b>

3.3. Experimental Setup .....	17
3.4.1. Production of microbeads using Polygalacturonic acid (PgA).....	18
3.4.2. Production of Alginate (Alg) based microbeads .....	18
3.4.3. Production of PgA based microbeads at pH 7 to optimize microbead diameter at 1500 rpm	18
3.4.4. Production of microbeads using various composition of Polygalacturonic acid (PgA) and Pectin .....	19
3.5. Viscosity measurement .....	19
3.5.1. Viscosity measurement of PgA solution at various concentration.....	19
3.5.2. Viscosity measurement of Alginate solution at various concentration .....	19
3.5.3. Viscosity measurement of various composition of Pectin and PgA solution.....	20
3.6. Hemolysis assay .....	20
3.7. Degradation study of microbeads.....	20
3.7.1. Degradation study of PgA based microbeads.....	20
3.7.2. Degradation study of Pectin and PgA based microbeads .....	21
3.8. Protein release study .....	21
3.9. Determination of surface topology of microbeads.....	21
3.10. FTIR analysis .....	22
3.11. Cell Culture .....	22
3.12. Microencapsulation of Macrophages (RAW 264.7) .....	23
3.13. Determination of encapsulation efficiency .....	23
3.14. Cell viability test using MTT .....	23
3.15. Visualization of encapsulated cells under inverted microscope.....	24
3.16. Cell cytotoxicity study using LDH Assay kit .....	24
3.17. Determination of ROS generation using NBT Assay .....	24
3.18. Visualization of encapsulated cells under confocal microscope .....	25
3.19. Morphological study .....	25
<b>Results and Discussion .....</b>	<b>26</b>
4.1. Optimization of diameter of PgA based microbeads .....	26
4.2. Viscosity of Alginate and PgA polymer solution at various concentration .....	28

4.3. Hemocompatibility of PgA based microbeads.....	28
4.4. Degradation study of PgA based microbeads .....	29
4.5. PgA based microbeads preparation at pH 7 .....	30
4.6. Optimization of diameter of Pectin and PgA based microbeads.....	30
4.7. Viscosity measurement of various composition of Pectin and PgA polymer solution ...	32
4.8. Hemocompatibility of Pectin and PgA based microbeads .....	32
4.9. Production of microbeads using three different polysaccharide-based polymers at 1500 rpm speed .....	33
4.10. Degradation study of PgA based microbeads .....	34
4.11. Protein release study .....	34
4.12. FTIR Analysis .....	35
4.13. Surface topology of Microbeads .....	36
4.14. Determination of encapsulation efficiency .....	37
4.15. Encapsulation of macrophages.....	38
4.16. Viability of encapsulated cells: MTT assay .....	39
4.17. Measurement of cell cytotoxicity: LDH assay .....	40
4.18. Superoxide assay: NBT reduction.....	41
4.19. Visualization of alive cells inside microbeads .....	42
4.20. Morphological study .....	43
<b>Conclusion .....</b>	<b>45</b>
<b>References.....</b>	<b>47</b>

# List of Figures

Figure 2.1: Polarization of un-activated macrophages to M1 & M2 phenotype. ....	12
Figure 2.2: Macrophage polarization pathways. ....	13
Figure 3.1: Holes were made on (a) 15ml centrifuge tube, and (b) 1ml syringe (30G needle diameter) using driller, to fabricate a centrifuge tube-syringe setup to produce microbeads. ....	16
Figure 3.2: Centrifuge tube-syringe setup (a) side view, and (b) top view. ....	17
Figure 3.3: Schematic of the experimental setup consisting of centrifugal platform and centrifuge tube-syringe setup in a swinging bucket .....	17
Figure 4.1: Microbead synthesized at 300 rpm using 2% (w/v) PgA solution (at pH 5). ...	26
Figure 4.3: Microbeads formed at (a) 1500 rpm, (b) 1700 rpm, (c) 1900 rpm using 7% (w/v) PgA solution (at pH 5); (d) 1500 rpm, (e) 1700 rpm, (f) 1900 rpm using 8% (w/v) PgA solution (at pH 5). ....	27
Figure 4.2: Representation of change in diameter of microbeads with respect to change in rotational speed and polymer concentration. ....	27
Figure 4.4: Representation of change in viscosity with the change in concentration of polymers including Alginate and PgA. ....	28
Figure 4.5: Hemolysis Percentage at different concentration of PgA solution. ....	29
Figure 4.6: Representation of change in the diameter of microbeads with respect to time. ....	29
Figure 4.7: Microbeads produced at 1500 rpm using (a) 7% and (b) 8% (w/v) Polygalacturonic acid (at pH 7). ....	30
Figure 4.8: Representation of change in diameter of microbeads with respect to change in rotational speed and polymer composition. ....	31
Figure 4.10: Representation of change in viscosity with respect to the polymer composition. ....	32
Figure 4.11: Hemolysis Percentage of different composition of Pectin and PgA based microbeads. ....	33
Figure 4.12: Microbead production using three different polysaccharide-based polymers. ....	33
Figure 4.13: Representation of decrease in diameter of microbeads with respect to time. ....	34
Figure 4.14: Representation of protein release study. ....	35

Figure 4.15: Representation of FTIR analysis: (a) Pectin; (b)PgA; (c) Pectin:PgA at 1:1 ratio, 10% (w/v) and (d) Pectin:PgA at 1:3 ratio, 10% (w/v).....	36
Figure 4.16: Inner structure of Microbead.....	36
Figure 4.17: Surface topology of Microbeads with different polymer concentration, (a) 9% (w/v)( Pectin:PgA at 1:1 ratio), (b) 9% (w/v)( Pectin:PgA at 1:3 ratio), (c) 10% (w/v)( Pectin:PgA at 1:1 ratio), (d) 9% (w/v)( Pectin:PgA at 1:3 ratio). ....	37
Figure 4.18: Representation of encapsulation efficiency. ....	37
Figure 4.19: Visualization of cell proliferation inside microbeads, under inverted microscope at 100X magnification (a) Day 1, (b) Day 3, (c) Day 5, (d) Day 7, (e) Day 9; and 400X magnification (f) Day9.....	38
Figure 4.20: Representation of effect on cell viability due to encapsulation. ....	39
Figure 4.21: Representation of percentage cell viability. ....	40
Figure 4.22: Representation of cell cytotoxicity level.....	41
Figure 4.23: Representation of activation of macrophages with respect to polymer composition. ....	42
Figure 4.24: Visualization of encapsulated macrophages in different composition of polymer, (a) 9%(w/v) (Pectin:PgA at 1:1 ratio), (b) 9%(w/v) (Pectin:PgA at 1:3 ratio), (c) 10%(w/v) (Pectin:PgA at 1:1 ratio), (d) 10% (w/v) (Pectin:PgA at 1:3 ratio) under confocal microscope. ....	43
Figure 4.25: Effect of anti-inflammatory environment on polarization of macrophages: Observation on day 5: (a) control, (b) cultured on 10% (w/v)( Pectin:PgA at 1:1 ratio), (c) 10% (w/v)( Pectin:PgA at 1:3 ratio); observation on day 7: (d) control, (e) culture on 10% (w/v)( Pectin:PgA at 1:1 ratio), (f) 10% (w/v)( Pectin:PgA at 1:3 ratio). ....	44
Figure 4.26: Representation of macrophage elongation with respect to polymer composition and time.....	44

# List of Tables

Table 2.1: General therapeutic modalities and their mechanism of action (MOA) for chronic wound healing .....	8
Table 2.2: Growth factors and its role in wound healing . ....	10
Table 2.3: Effects of growth factors and cytokines in wound repair .....	11
Table 4.1: Tabulation of an approximate number of alive cells in each microbead.... .....	42

# Chapter 1

## Introduction

### 1.1. Chronic Wound

Wounds, which fail to get repaired through the orderly process of healing within a stipulated timeframe, are characterized as chronic wounds. Even after three months, wound bed lacks to produce structural and functional integrity through healing, in the case of chronic wound [1]. Most of the time presence of a raised, hyperproliferative, yet non-advancing characteristics of wound area helps to identify chronic wounds. One of the major reasons for this failure to heal is uncontrolled and self-sustaining inflammatory environment. Moreover, wound healing is an inherently complex procedure, which is the main cause of the failure of monotherapies [2]. The local wound environment remains mostly rich in pro-inflammatory cytokines. Moreover, this leads to an imbalanced enzymatic milieu consisting of an excess of matrix metalloproteases (MMP) and reduces their inhibitors, which lead to the destruction of the extracellular matrix (ECM). Thus, the healing process is delayed due to profound inflammation and this can be depicted as a hallmark of chronic wounds. Understanding of molecular mechanism of wound healing is necessary to control this prolonged inflammation, also to repair tissue within stipulated time. Recent scientific advancement has come up various new approaches to cure this problem of chronic wound like the application of akin substitutes, growth factors and stem cell-based therapy [3].

### 1.2. Wound Healing

Wound healing is a complex process of revitalization of impaired tissue layer and damaged cellular structure [4]. There are **six stages of wound healing** according to the study published in the World Journal of Surgery, each of which is very crucial and depends on one another in order to completely heal a wound.

- a) **Rapid hemostasis:** This is the first stage of healing where bleeding is terminated, because of vasoconstriction.

- b) **Inflammation:** Inflammation acts as an alert system. Beyond that, it also helps the system to lead the healthy cells, where those cells should be headed next. Hence, inflammation is one of the vital stages of wound healing. However, prolonged inflammation can actually hinder the regeneration process.
- c) **Proliferation and migration:** During inflammation, various stimuli causes migration and proliferation of various cells engaged in the healing process. Migration is a coordinated process, which involves the movement of cells in a specific order and proliferation is similar to hemostasis because in this case cells toil to constrict the blood vessels.
- d) **Angiogenesis:** Body starts to rebuild tissue once the bleeding is under control. Meanwhile, new blood vessel formation occurs, which process known as angiogenesis. This process helps to replace damaged arteries and veins by following a complex mechanism.
- e) **Reepithelialization:** Once veins have regrown, reepithelization occurs. This process creates several layers which prevent fluid loss from the wound bed and offers protection.
- f) **Synthesis:** This is the last step of wound healing but it often occurs simultaneously with other steps of healing. Here, certain proteins help in clotting of blood which is followed by formation of new veins and skin due to angiogenesis and remodeling of collagen respectively.

Furthermore, each of these six stages is very crucial and also interdependent on each other in order to heal a wound completely [5]. Therefore, generation of any effective therapy for pathological tissue repair requires a complete understanding of those mechanisms, which control these above-mentioned six stages of wound healing [3].

### 1.3. Factors Affecting Wound Healing

Patients in India do not receive proper care due to the limitation of resources and huge expense of medical treatments. This critical condition also adds to the development of chronic wounds. Healthcare costs have been steadily increasing worldwide. It has been reported, that in India funding in public healthcare is not more than 5% of the annual GDP (gross domestic product). Hence, a majority of the population (approximately 80%) met



healthcare costs from out-of-pocket payments [6]. Three major causes of this chronic wound development are deficient healthcare services, insufficient workforce, inadequate and low-grade health care infrastructure [7]. Apart from these, comorbidities such as Peripheral vascular disease (PVD) and diabetes mellitus (DM) alter the wound healing process; act as an additional factor in the development of a chronic wound. Diabetes affects wound healing through the development of ischemia, decreased inflammatory responses, loss of protective sensations due to neuropathy, and increased the threat of infection. Whereas PVD can cause morbidity and mortality, especially in aged and diabetic populations [6].

Systemic factors that have influencing effect on wound healing are [8]:

- Diabetes
- Age
- Sex Hormones in Aged Individuals
- Stress
- Obesity
- Medications (e.g., Glucocorticoid Steroids, Non-steroidal Anti-inflammatory Drugs, Chemotherapeutic Drugs)
- Smoking
- Alcohol Consumption
- Poor circulation and Perfusion
- Venous stasis
- Infection
- Trauma/repetitive forces
- Pressure
- Immunosuppression
- Malnutrition

Apart from these external factors, various cells are responsible for proper wound healing such as macrophages, neutrophils, keratinocytes, endothelial cells, fibroblasts, and lymphocytes. If these cells do not carry out their functions properly in a harmonic manner, healing does not follow its stages in correct order. Multiple local, as well as systemic factors, cause impaired wound healing by affecting one or more individual phases [8].

## 1.4. Objectives

- II. Fabrication of a low-cost experimental setup, to produce microbeads for cell encapsulation.
  - Optimization of the rotation speed of centrifuge.
  - Optimization of the polymer composition, suitable for cell encapsulation.
- III. Development of biocompatible microbeads with anti-inflammatory properties.
  - Determination of hemocompatibility of selected polymer(s).
  - Determination of post-encapsulation cytotoxicity level inside microbeads.
- IV. Encapsulation of macrophages in Pectin and PgA based microbeads.
  - Determination of cell viability inside microbeads.
- V. Evaluation of the efficiency of microbeads in the polarization of un-activated macrophages to elongated M2 phenotype.

## Chapter 2

# Review of Literature

### 2.1. Application of Stem Cells in Chronic Wound Healing

Current treatments available for chronic wound healing such as special type of wound dressing, hydrogels or scaffold-mediated delivery of growth factors (e.g., TGF- $\beta$ , bFGF), have not yet achieved the desired results. Therefore, more effective therapeutic approaches are required. It has been reported that wound healing can be regulated by bone marrow-derived mesenchymal stem cells (BMSCs) through a series of paracrine growth factors [9]. BMSCs can be induced to differentiate into effector cells involved in wound healing, such as keratinocytes, fibroblasts, and endothelial cells. Thus, stem cells help to accelerate wound closure and enhance vascularization, granulation, reepithelialization, and tissue formation [10]. Recent histology and immunohistochemistry results have shown that hydrogel laden BMSCs can be a promising therapeutic strategy for the management of diabetic ulcers. This promotes angiogenesis, extracellular matrix (ECM) secretion, granulation tissue formation, reepithelialization, rapid wound bed contraction, and regeneration of sebaceous glands as well as hair follicles. Thus, it contributes to rapid skin wound healing of diabetic patients with reduced scar formation. This series of beneficial biological effects occur because it enhances secretion of TGF- $\beta$  and bFGF. These results have provided a reliable guidance in clinical settings for the treatment of diabetic foot ulcer [11]. Several groups of scientists have conducted various experiments to define optimum time required for these steps and suitable route of administration. However, to define these we need to understand MSCs mechanism of action (MOA) in repairing of tissue and its regeneration process. Large-scale multicenter trials need to be performed to test MSC-based therapy stringently, to completely validate this for any commercial purpose [12]. MSCs have shown highest efficiency in promotion of chronic wound healing as compared to other therapies. Further, comparative studies have demonstrated that intradermal injection is more effective than systemic injection of MSCs in chronic wound healing purpose. Intradermal injection of MSCs can promote rapid cell proliferation, granulation tissue formation, angiogenesis and collagen fiber synthesis [13]. Compared to either intravenous or topical administration of BMSCs, BMSC aggregate

transplantation showed better neo-vascularization and more regular collagen deposition on acute cutaneous wound model, thus bringing higher regenerative and healing efficacy. The mechanism behind this may be better regulation of inflammatory process due to BMSC aggregate engraftment [14]. It has been demonstrated by various clinical trials that mesenchymal stem cells (MSCs) not only help to decrease inflammatory response, promote angiogenesis, enhance closure of wound but also increase tensile strength within the wound. However, the regenerative ability of MSCs in human wounds has not yet been tested, because of various limitations in human studies. Further research is required to propose an optimized method to isolate, characterize and harvest stem cells indisputably [12].

## **2.2. Application of Peptides in Chronic Wound Healing**

Other than administration of stem cells, rapid wound healing can be achieved by using camel milk Peptide (CMP) as a therapeutic agent. It is an effective immune stimulant and antioxidant, which induces oxidative stability by enhancing the activity of some major antioxidant enzymes such as catalase (CAT), glutathione (GSH), and superoxide dismutase (SOD). Thus, CMP speeds up wound healing by acting as a potential adjuvant in improving chronic wound healing in those with diabetic conditions [15].

## **2.3. Application of Peptides in Chronic Wound Healing**

A major component of most skin substitutes is collagen because of its bioactive cues and specific structure. Thus, either collagen or collagen mimetic protein can be used to treat the chronic wound. Scl2GFPGER, a collagen mimetic protein, can be encapsulated in a bioactive hydrogel, to promote active wound healing. Further, a redesigned Scl2GFPGER, engineered collagen (eColGFPGER), reduces steric hindrance of integrin-binding motifs. Thus, it increases the overall stability of the triple-helical backbone which leads to increase in cell adhesion to substrates. Collagen-mimetic wound dressing Permits controlled modulation of cellular interactions and degradation rate without affecting other physical properties. Moreover, a bioactive dressing can be provided by its fabrication into uniform hydrogel microspheres which can readily conform to irregular wounds [16]. Calcium alginate is a natural polymer which helps in wound healing, which possesses

faster epithelialization though it has a milder inflammation effect while implemented inside the system. Calcium alginate also has excellent cytocompatibility as well as histocompatibility

characteristics and it acts as a promoter of diabetic wound healing by attenuating inflammatory reaction and increasing the contraction of wounds. It increases the levels of type I collagen and hydroxyproline which leads to a significant increase in the tensile strength of wound. All in all, the stimulation of expression of collagen I and elevation of collagen I to III ratios to a large extent are major causes of this accelerating effect of calcium alginate. Thus calcium alginate based dressing provides a potential strategy of wound healing and easily used way to ameliorate the foot ulceration by preventing limb amputation in diabetic populations [17]. Other than natural polymers some synthetic polymers also help in wound healing process. Prolonged insulin release to the target site can be provided by insulin-secreting cells encapsulated into Pectin-GDA hydrogel microsphere. The basis of this prolonged release is the prevention of immune clearance and migration because of microsphere encapsulation. Thus keeping the microencapsulated cells in the desired location. This combination of insulin-releasing cells and Pectin-GDA hydrogel microencapsulation is a novel method for delivering a steady and constant dose of insulin to wound site [18]. Pectin is the major component of plant cell walls which displays diverse biological activities such as immunomodulation. The macromolecule of Pectin contains fragments of both linear and branched regions of polysaccharides such as homo-galacturonan, apio-galacturonan, xylo-galacturonan, and rhamno-galacturonan-I. These structural features of Pectin are key to its effect on the immune system. The backbone of Pectin macromolecule has immunosuppressive activity. Macrophage activity can be decreased and delayed-type hypersensitivity reaction can be inhibited by the Pectin containing greater than 80% galacturonic acid residue. Whereas biphasic immunomodulatory action can be attained by the help of branched galacturonan fragments [19]. Pectic acid is also known as Polygalacturonic acid have anti-inflammatory property besides its bioadhesive property. Furthermore, in this anti-inflammatory environment macrophages might have a higher probability to polarize in M2 phenotype. Hence, Pectin or Pectic acid can be used to treat chronic wounds by encapsulating growth factors, signaling molecules, stem cells or macrophages and delivering those bioactive factors at the target site [20].

Table 2.1: General therapeutic modalities and their mechanism of action (MOA) for chronic wound healing (adapted from, [12]).

Treatment	Proposed Mechanism(s) of Action
<b>Debridement (variety of methods)</b> a) Surgical b) Chemical	Removes foreign debris and devitalized or contaminated tissues from the wound bed.
<b>Compression</b>	Decreases venous backflow and capillary leakage.
<b>Negative Pressure</b>	Removes exudate, reduces edema, increases local Perfusion, decreases bacterial count, and enhances granulation tissue formation.
<b>Electrical Stimulation</b>	May promote migration of various cell types to the wound by reducing the size of venous leg ulcer.
<b>Hyperbaric oxygen therapy (HBOT)</b>	Improves neovascularization, reduces production of pro-inflammatory cytokines, and increases synthesis of GFs and collagen.
<b>Lasers, phototherapy, shockwaves, and ultrasound</b>	Decreases inflammatory cells, increases fibroblast proliferation, stimulates angiogenesis, promotes the formation of granulation tissue, and increases collagen synthesis.
<b>Silver</b>	Antimicrobial
<b>Cadexomer iodine</b>	Antimicrobial
<b>Others (povidone-iodine, Peroxide preparations, ethacridine lactate, or chlorhexidine)</b>	Antimicrobial
<b>Dressings (alginate, foam dressing, hydrocolloids, hydrogels)</b>	Provides appropriate moist wound environment, which contributes to faster wound reepithelization.

## 2.4. Application of Growth Factors in Chronic Wound Healing

Several growth factors (GFs) help in the rapid healing of wound bed such as acidic Fibroblast growth factor (aFGF), Platelet-derived growth factor (PDGF) (Table 1). Furthermore, administration of aFGF on a diabetic patient, significantly improve healing of wound bed. The therapeutic application of aFGF has its own limitation of shorter halflife and very low efficiency of delivery. Transactivator of transcription protein (TAT) mediated delivery of aFGF helps to overcome this limitation. Moreover, it helps in chronic wound healing by facilitating Penetration of aFGF through the epidermis. TAT has been tagged with this feature because it has a regulatory effect on expression of  $\alpha$ -SMA, restoration of TGF- $\beta$ 1 and TGF- $\beta$ R2 synthesis. This TAT-mediated aFGF delivery has the capability to prove itself as a less invasive and more efficient approach, in the case of type 1 diabetic patient (T1DM), having ulcers due to any physical damage or the diabetic condition [12]. Among T1DM patients, the major cause of delay in wound healing is decreased in the number of regulatory T cells (Treg), and cytokine such as interleukin 2 (IL-2). Prolonged inflammatory phase act as a hallmark in the case of chronic wounds such as diabetic foot ulcer. IL-2 topical cream can be beneficial in the treatment purpose of diabetic foot ulcer

[21]. This is suitable for patients from any age group and background since much education or advice from expertise is not required in the application of the topical cream. Moreover, topical cream has its own benefits over intravenous treatment such as thin line chances of infection and allergic reactions. This treatment method also helps to protect skin from issues like dryness, by maintaining a moist environment around the wound bed. Other than this above-mentioned cytokine, IL-17 may have some regulatory functions in the healing of chronic wounds by influencing the differentiation of macrophages into CD11b+Ly6C+MHC Class II+ [22]. Other than aFGF, due to injury huge amount of degranulating platelets release PDGF during the early stage of injury [23]. Furthermore, the presence of PDGF has been observed in samples collected from the wound site of pig, murine and human [24]. It has been observed, that PDGF receptors are present in dermis whereas ligands are available in the epidermis. This observation suggests that PDGF and its receptor follows paracrine mechanism. Some experimental results have shown decrease in expression of PDGFs and its receptors during diabetic condition, which leads to the formation of the chronic wound [25]. This evidence suggests that a proper wound healing

requires a certain level of expression of this above-mentioned growth factor. In addition to aFGF and PDGF, a considerable amount of Epidermal growth factor (EGF) and TGF was also present in wound fluid collected from burn injuries [26]. Further, studies have shown the key role of Heparin-binding EGF (HBEGF) in granulation tissue formation and reepithelialization. The highest amount of HB-EGF is present during the stage of the proliferation of keratinocytes [27].

Table 2.2: Growth factors and its role in wound healing (adapted from, [12]).

Treatment	Mechanism(s) of Action
<b>PDGF</b>	For diabetic foot ulcer (DFU), this provides a scaffold on which new cells can migrate and attach.
<b>bFGF</b>	This promotes the proliferation of fibroblasts and capillary formation and accelerates tissue regeneration.
<b>rhEGF</b>	For both DFU and venous chronic wounds. Increases granulation tissue formation and reduces wound and cellulitis in the surrounding area.

## 2.5. Application of Cytokines in Chronic Wound Healing

Cytokines are synthesized as well as secreted by various cell types present in our system. These are mainly small proteins or glycoproteins, which helps in regulation of various activities of the cell (e.g., growth and differentiation), matrix synthesis, migration of cells, and immune functions through binding to target cells with the help of specific receptors [28]. Wound healing is a complex process which follows the stages of inflammation after initial injury, tailed by cell proliferation and migration of parenchymal as well as mesenchymal cells, then production and deposition of extracellular matrix (ECM) [29]. If wound bed fails to follow this orderly process then fibrosis occurs. At the latter stage, cellular interaction takes place via a complex network of cytokines. This leads to immense remodeling and heightened production of ECM, followed by abnormal deposition in the tissue. Each and every cytokine have its own role in both promotion and inhibition of fibrogenesis. Progress in the understanding of the process, responsible for pathogenesis of




fibrosis, provides us the knowledge to generate inhibitors of these profibrogenic cytokines and GFs. Further, those inhibitors can play the role of novel therapeutic agents to control undesirable fibrosis [30]. Proinflammatory cytokines such as IL-6, IL-1 $\alpha$ , IL-1 $\beta$ , TNF- $\alpha$  are upregulated during inflammatory phase [31]. A major source of these cytokines are macrophages and polymorphonuclear leukocytes. For normal repairing system of the wound, a balanced expression of these cytokines is required [32]. Other than proinflammatory cytokines, Anti-inflammatory cytokines such as IL-10 also have a significant role in the regulation of wound repair. IL-10 plays a significant role in limiting and terminating inflammatory response at the injury site and inhibits the formation of a scar. Apart from that, this cytokine has also shown key role in differentiation and growth of endothelial cells, immune cells, and keratinocytes. Experimental results suggest treatment with IL-10 results in scar-free healing [33].

Table 2.3: Effects of growth factors and cytokines in wound repair (adapted from, [34]).

Process	Growth Factors and/ or Cytokines Involved
<b>Neutrophil infiltration</b>	MCP-1, IL-8, IL-10, TGF- $\beta$
<b>Macrophage infiltration</b>	TGF- $\beta$ , IL-10, MCP-1, MIP-1 $\alpha$
<b>Angiogenesis</b>	FGF2, VEGF-A, GM-CSF, PLGF, Angiopoietins, Cyr61, MCP-1, IL-8, IP-10, HGF
<b>Fibroplasia</b>	TGF- $\beta$ , CTGF, IGFs, PDGF, GM-CSF
<b>Matrix deposition</b>	TGF- $\beta$ , Activin, CTGF, Cyr61, NGF, IGF-1, FGF2
<b>Scarring</b>	IL-6, TGF- $\beta$ , CTGF, IL-10, Activin, IGF-I
<b>Reepithelialization</b>	EGF, FGF2, FGF7, FGF10, IGFs, IL-6, TGF- $\beta$ , IP-10, TGF- $\alpha$ , Activin, Leptin, HB-EGF, BMP-6, GM-CSF, NGF

## 2.6. Application of Macrophages in Chronic Wound Healing

Macrophages are typically known for their role in immune defence mechanism and phagocytic capabilities. Recently, some well-established evidence have demonstrated heterogeneous characteristics of un-activated macrophages. One possible explanation could be the ability of un-activated macrophages to polarize into two different phenotypes (e.g., pro-inflammatory and anti-inflammatory) in response to the various microenvironmental stimulus. Activated macrophages which are polarized into anti-inflammatory phenotypes, play a crucial role in wound healing [35]. Two well-known macrophage polarization process activates unactivated macrophages to pro-inflammatory phenotype (M1), activated through classical pathway or anti-inflammatory/ wound healing phenotypes (M2a, M2b, M2c, M2d), by following alternative pathway, in response to various environmental stimuli such as Interferon gamma ( $\text{IFN}\gamma$ ) and Interleukin-4 (IL-4), respectively [36, 37].



Polarizing stimulus	$\text{IFN-}\gamma$ , LPS, $\text{IFN-}\gamma$ +LPS	IL-4, IL-13, Ic, IL-10, GC, GC+TGF $\beta$
Phenotype	Proinflammatory	Anti-inflammatory
In vitro morphology	Round/oval	Elongated, fibroblast-like
Products/Markers	TNF $\alpha$ , IL-1 $\beta$ , IL-6, IL-12, IL-23, CXCL10, pSTAT1, MMP9	IL-10, TGF $\beta$ , CCL17, CCL22, CD163, CD206, pSTAT3/6
Phagocytic activity	High	Low
Antigen presentation	High	Low
Arginine metabolism	iNOS: Arginine $\rightarrow$ NO	Arg1: Arginine $\rightarrow$ Ornithine
Antibacterial capacity	High	Low
Effect on tumors	Tumoricidal	Protumorigenic

Figure 2.1: Polarization of un-activated macrophages to M1 & M2 phenotype (adapted from [38]).

The M1 phenotype induces production of pro-inflammatory cytokines such as IFN-  $\gamma$ , Interleukin-2 (IL-2), Tumor necrosis factor alpha (TNF- $\alpha$ ) and some microbicidal agents like reactive oxygen species (ROS) and nitric oxide (NO) [38, 39]. On the other hand, in later stages of tissue repair and healing process M2 phenotype predominates by enhancing the secretion of anti-inflammatory cytokine Interleukin-10 (IL-10) and growth factors like vascular endothelial growth factors (VEGF) and transforming growth factor beta (TGF $\beta$ ) [40]. M1 and M2 macrophages can be distinguished by examining the ratio of IL-12 and IL-10 [41]. Macrophage polarization is an important part of effective wound healing. Each phenotype of macrophages have its own distinct role in this healing process such as M2d phenotype has a critical role in angiogenesis during the healing process. Some transcription factors (TFs) play a key role in activation of macrophages, for example, IRF5 TF activates un-activated macrophages into M1 phenotype and Jumonji domain containing-3-IRF4 is responsible for activation of M2 phenotype [35].

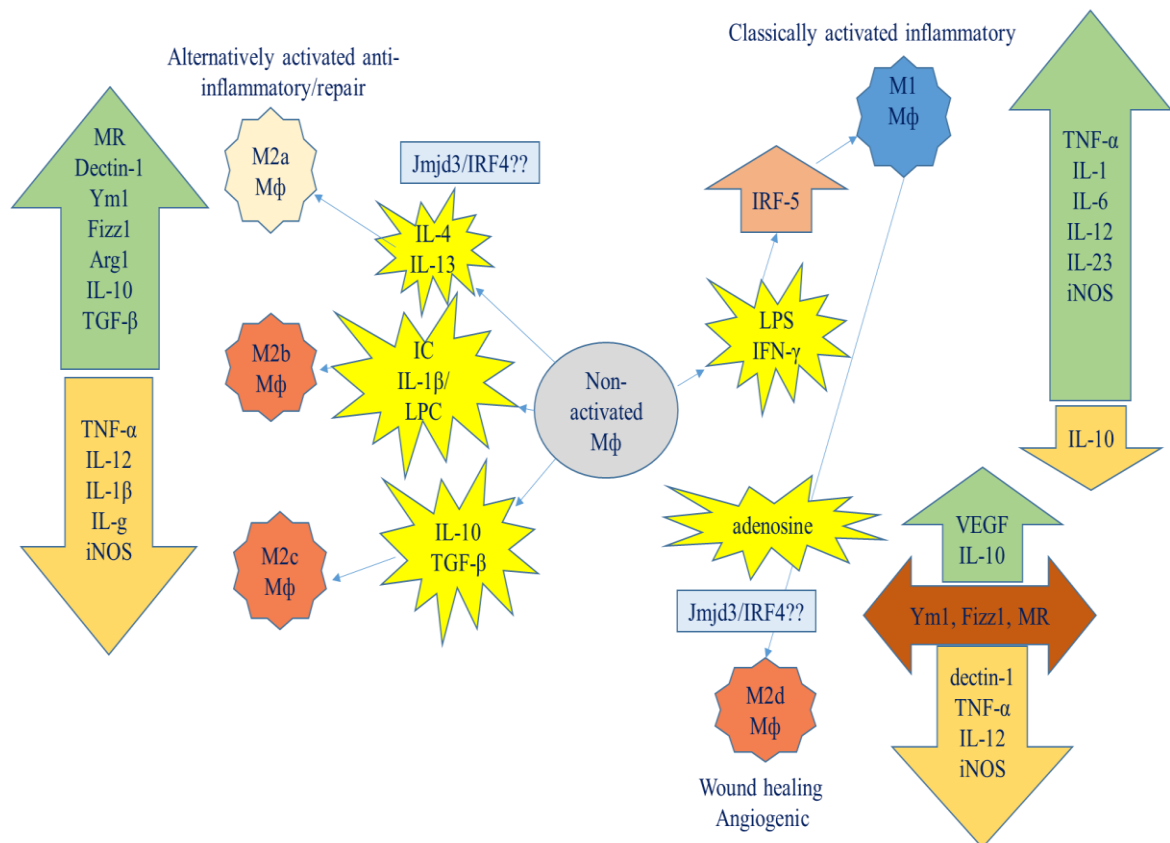


Figure 2.2: Macrophage polarization pathways (adapted from [35]).

The progress in the field of regenerative medicines and tissue engineering (TE) have made it possible to produce desired biomaterials, having tailored mechanical, physical, chemical and temporal characteristics required to interact with the host system. Such advancement in the functionality of biomaterials and understanding of macrophage response mechanism have made it possible to identify and select the suitable design of biomaterials, which can control response of host system. Thus, desired characteristics of biomaterials can help us to attain successful tissue engineering [42]. In this case of chronic wound healing, immune-informed biomaterials can be designed for sustainable release of some desired factors (e.g., IL-4, IL-10, steroids) to control the immune response. This strategy would help in the direct polarization of macrophages to wound healing phenotype by overcoming native signaling pathways [43, 44]. Incorporation of gene delivery vectors, small molecule drugs (e.g., steroids), desired cytokines producing cells (e.g., M2 phenotype of macrophage), growth factors (e.g., PDGF, aFGF), into a controlled systems could help in the release of single factor or multiple factors in a sustainable manner [44]. The selective polarization of macrophages requires complete understanding of biomaterial cues. Moreover, it will help us to design new generation 'immuno-informed' biomaterials to interact with the immune system as necessary for post-implantation macrophage response, in the case of chronic wound healing [42].

## **2.7. Application of microencapsulation of cells in chronic wound healing**

Cell encapsulation for immune-isolation is a method, which enables the process of continuous and long-term delivery of therapeutic factors into a selected target tissue. The encapsulated cells help to produce and release therapeutic molecules when transplanted into the body [45]. The principle of cell encapsulation is the isolation of transplanted cells from its surrounding host immune system by enclosing them in a semipermeable polymeric matrix. The main purpose of this semipermeable membrane is to exclude harmful components of host immune system such as immunoglobulins, complement and immune cells to prevent immune rejection after transplantation into the host system. Furthermore, this semipermeable membrane also allows bi-directional diffusion of oxygen, nutrients, waste and the therapeutic products to maintain the encapsulated cells viably, healthy and functional. In addition to this, cell encapsulation offers an internal matrix to the cells that create a 3D microenvironment for the encapsulated. This internal

matrix act as a substitute for the ECM of native tissues, which is important to keep the encapsulated cells viable and functional [46]. Incorporation of immunomodulatory human mesenchymal stromal cells (hMSCs) has been Performed, in animal models to reduce secondary inflammatory responses. This therapeutic protocol can be useful for the treatment of spinal cord injury (SCI). Thus, limitations in direct hMSC implantation can be circumvented, in post-SCI treatment. Alginate microencapsulation is mostly used by a different group of scientists as an implantable vehicle for delivery of hMSCs to the wound bed. Encapsulated hMSCs remains viable and its secretory functions also do not get affected if the encapsulation is carried out in a proper manner. Further, modulation of the functions of inflammatory macrophages can be attained both in *in-vitro* and *in-vivo*, even if hMSC and macrophages are not in direct contact. Induction of hMSCs with anti-inflammatory factors such as IL-4, enhance secretion of anti-inflammatory cytokines. Thus, this process helps to promote activation of more number of the M2 phenotype. *In-vitro*, this was evident after observing a reduction in expression of iNOS by macrophages with a collateral increase in CD206, a marker for M2 macrophages [47].

## 2.8. Rationale of current study

Procurement of macrophages from peripheral blood is much easier than the complex process of collection and processing of hMSCs. Moreover, efficient delivery of macrophages would also help to maintain a proper balance in between pro-inflammatory and anti-inflammatory environment by secreting desired cytokines and growth factor at the wound bed while applied *in vivo*. Major challenges in implementing such strategy are: prevention of macrophages from washing out from the site of injury and sustenance of M2 phenotype over the period of healing. This limitation could be overcome by encapsulation of macrophages in micro-bead system. Further, use of such polymers which have anti-inflammatory properties (e.g., pectin and PgA) might help us to achieve our goal, by polarizing macrophages to M2 phenotype. Those encapsulated M2 phenotypes would secrete anti-inflammatory cytokines (e.g., IL-10) and growth factors (e.g., VEGF) in a sustainable and controlled manner, which would speed up the healing process. Hence, we envisioned that the application of encapsulated macrophages could be used for rapid and scar free healing of chronic wounds.

## Chapter 3

# Materials and Methods

### 3.1. Materials

Pectin, Calcium Chloride (Anhydrous) and Tween-80 were obtained from HiMedia. Polygalacturonic acid (PgA) was purchased from Sigma-Aldrich. 15 ml Falcon tube was purchased from Tarson and 1ml syringe (needle diameter 30 gauge) fabricated by the company Terumo, was bought from a local pharmacy. RAW 26.7 cell line was obtained from NCCS, Pune. Materials used in cell culture purpose such as Phosphate buffer saline (1X), DMEM cell culture media (Low glucose), Foetal bovine serum (FBS), Trypan blue (Powder), Antimitotic antibody, MTT (Thiazolyl Blue Tetrazolium Bromide) and Nitro Blue Tetrazolium Chloride (NBT) Dye were purchased from HiMedia. Lactate Dehydrogenase (LDH) Assay Kit was purchased from Accurex. Cell culture equipment such as T-25, T-75 Flasks, and cell scrapers were purchased from HiMedia.

### 3.2. Fabrication of centrifuge tube-syringe setup

Using driller machine, 20 centrifuge caps were holed as shown in fig. 2(a). Then holes were made on both sides of 1 ml syringe as shown in fig. 2(b). This was done for 20 number of the 1 ml syringe. Then syringe was inserted into a hole made in centrifuge caps. At the end, centrifuge cap was inserted into centrifuge tube to make the complete setup as shown in fig. 2(c, d).



Figure 3.1: Holes were made on (a) 15 ml centrifuge tube, and (b) 1 ml syringe (30G needle diameter) using driller, to fabricate a centrifuge tube-syringe setup to produce microbeads.

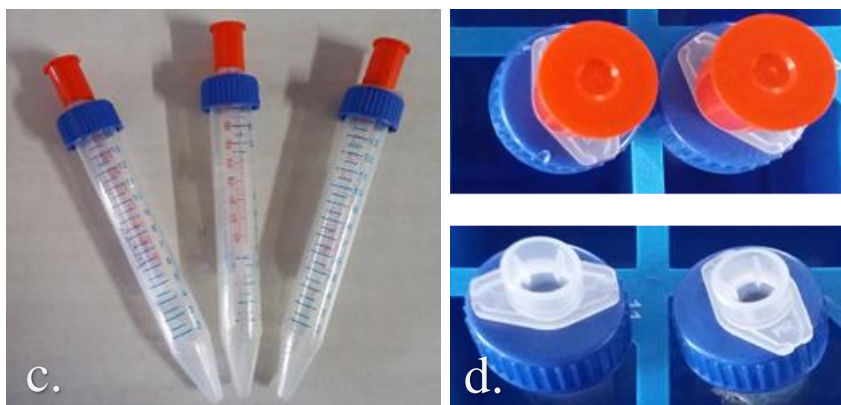


Figure 3.2: Centrifuge tube-syringe setup (a) side view, and (b) top view.

### 3.3. Experimental Setup

In this novel, rotor based set-up, droplets were generated within the dripping regime at the micro-nozzle tip of a commercially available syringe. The syringe contains polymer solution and centrifuge tube contains  $\text{CaCl}_2$  solution. Therefore, the Pectin and PgA polymer droplets impact perpendicularly to the air-liquid meniscus inside the centrifuge tube. Gravity prevails to realign those centrifuge tubes in a vertical position when the rotor halts. Further processing (e.g., culturing or analysis) could be done once the Centrifuge tube-syringe setup is taken out from the rotor. Several nozzles could be operated on the same rotor simultaneously, due to the intrinsic rotational symmetry induced artificial gravity conditions (adapted from B.Tech thesis work conducted by Mr. Rahul Kumar at NIT- Rourkela, titled: Fabrication of micro-alginate beads under centrifugally induced artificial gravity conditions).

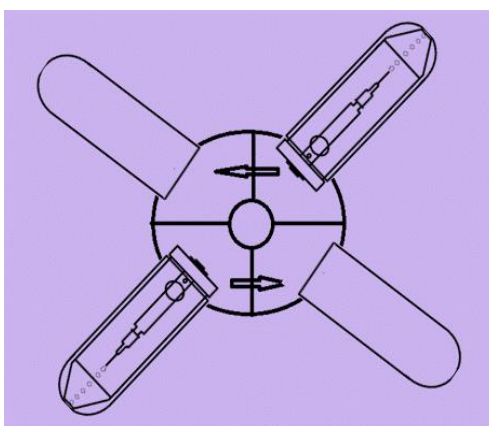


Figure 3.3: Schematic of the experimental setup consisting of centrifugal platform and centrifuge tube-syringe setup in a swinging bucket

### **3.4. Production of microbeads**

Microbeads were produced using various concentration of Polygalacturonic acid (PgA) and Pectin at a different proportion to optimize the microbead diameter at different rotational speed.

#### **3.4.1. Production of microbeads using Polygalacturonic acid (PgA)**

PgA solution was prepared within the range 2% to 8% (w/v) in distilled water. This was followed by preparation of 100 mM  $\text{CaCl}_2$  + 0.1% (v/v) Tween-80 solution. The pH of the polymer solutions was adjusted to 5 using pH meter. In the experimental setup, the syringe was loaded with 200  $\mu\text{l}$  of the polymer solution and centrifuge tube contained the 1.5 ml  $\text{CaCl}_2$  solution. Due to centrifugal force polymer solution came out in a drop by drop manner through the 30G needle and crosslinked in  $\text{CaCl}_2$  solution. The rotation speed was varied within a range of 300 rpm to 1900 rpm with an interval of 200 for each concentration of PgA solution.

#### **3.4.2. Production of Alginate (Alg) based microbeads**

2% Alginate solution, 100mM  $\text{CaCl}_2$  + 0.1% (v/v) Tween-80 solution was prepared in distilled water. In the experimental setup, the syringe was loaded with 200  $\mu\text{l}$  of the polymer solution and centrifuge tube contained the 1.5 ml  $\text{CaCl}_2$  solution. Due to centrifugal force polymer solution came out in a drop by drop manner through the 30G needle and crosslinked in  $\text{CaCl}_2$  solution. Moreover, the rotational speed-regulated the diameter of the microbeads. At 1500 rpm centrifugation speed microbeads were synthesized using swinging bucket centrifuge (REMI, 4M). Prepared beads were visualized under 10X magnification using an inverted microscope (Zeiss).

#### **3.4.3. Production of PgA based microbeads at pH 7 to optimize microbead diameter at 1500 rpm**

7% and 8% (w/v) PgA solution was prepared in distilled water and pH were adjusted to 7 using pH meter. This was followed by preparation of 100 mM  $\text{CaCl}_2$  + 0.1% (v/v) Tween-80 solution. In the experimental setup, the syringe was loaded with 200  $\mu\text{l}$  of the polymer solution and centrifuge tube contained the 1.5 ml  $\text{CaCl}_2$  solution. Due to centrifugal force polymer solution came out in a drop by drop manner through the 30G needle and



crosslinked in  $\text{CaCl}_2$  solution. The rotation speed was maintained at 1500 rpm for both the polymer concentration.

#### **3.4.4. Production of microbeads using various composition of Polygalacturonic acid (PgA) and Pectin**

9% and 10% (w/v) solution of Pectin and PgA was prepared and 9% Pectin and PgA solution were mixed 1:1 and 1:3 ratio respectively and a similar proportion was also maintained for 10% solution of Pectin and PgA. The pH of these solutions was adjusted within a range of 7.2-7.4 using pH meter (Systronics). 100 mM  $\text{CaCl}_2$  solution with 0.1w% Tween-80 was made to prepare the microbeads because of polymerization in  $\text{CaCl}_2$  Solution. In this experimental setup, the syringe contains 200  $\mu\text{l}$  of the polymer solution and centrifuge tube contains the 1.5 ml  $\text{CaCl}_2$  solution. Due to centrifugal force polymer solution come out in a drop by drop manner through 30G needle and crosslinks in  $\text{CaCl}_2$  solution. Moreover, the rotational speed regulates the diameter of the microbeads. Hence, three set of experiments were conducted at 1500 rpm, 1700 rpm and 1900 rpm using swinging bucket centrifuge (REMI, 4M) to optimize the microbead diameter. Prepared beads were visualized under 10X magnification using an inverted microscope (Zeiss) and the diameter of beads was determined using ImageJ software.

### **3.5. Viscosity measurement**

The viscosity of various polymer solution was measured with the help of viscometer.

#### **3.5.1. Viscosity measurement of PgA solution at various concentration**

Viscosity measurement of PgA solution at various concentration: PgA polymer solution was prepared within the range 2% to 8% (w/v) in distilled water and pH was adjusted to 5 using pH meter. The viscosity of each sample was determined using viscometer (BOHLIN VISCO).

#### **3.5.2. Viscosity measurement of Alginate solution at various concentration**

Alginate solution was prepared within the range 2% to 6% (w/v) in distilled water. The viscosity of each sample was determined using viscometer (BOHLIN VISCO).

### 3.5.3. Viscosity measurement of various composition of Pectin and PgA solution

9% and 10% (w/v) solution of Pectin and PgA was prepared and 9% Pectin and PgA solution were mixed 1:1 and 1:3 ratio respectively and a similar proportion was also maintained for 10% solution of Pectin and PgA. The pH of these solutions was adjusted within a range of 7.2 to 7.4 using 1 M NaOH. The viscosity of these four samples was determined using viscometer (BOHLIN VISCO).

## 3.6. Hemolysis assay

For the hemolysis assay, Anticoagulated blood was diluted using 0.9% NaCl (physiological saline) in the ratio 8:10, to prepare the stock solution. The beads were prepared using 7% and 8% (w/v) PgA concentration (at pH 5) and the combination of Pectin and PgA (at 9% as well as 10%) in a ratio 1:1 and 1:3 respectively (at pH 7). The microbeads were placed into 15 ml falcon tubes and 0.5 ml of diluted blood was dispensed on them. The volume inside the tubes was made up to 10 ml using 0.9 % NaCl. 0.5 ml of diluted blood was added in a falcon tube and the volume was made up to 10 ml by using saline, and this was taken as the negative control for this experiment. The positive control was prepared by adding 0.5 ml of diluted blood and 0.5 ml of 0.01 M HCl and making up the volume to 10 ml using saline. All the tubes were centrifuged at 4000 rpm for 10 mins. OD of the supernatants was measured at 540 nm with the help of spectrophotometer [36]. Hemolysis Percentage was calculated using the following formula:

$$\text{Hemolysis \%} = \frac{OD_{\text{test}} - OD_{\text{negative control}}}{OD_{\text{positive control}} - OD_{\text{negative control}}} \times 100$$

## 3.7. Degradation study of microbeads

Microbeads were prepared using various composition of polymers. Washing of microbeads was followed by resuspension of those in PBS for the desired time span to check any degradation is occurring or not.

### 3.7.1. Degradation study of PgA based microbeads

7% to 8% (w/v) PgA solution was prepared in distilled water. This was followed by preparation of 100 mM CaCl<sub>2</sub> + 0.1% (v/v) Tween-80 solution. The pH of the polymer

solutions was adjusted to 5 using 2 N NaOH. In the experimental setup, the syringe was loaded with 200  $\mu$ l of the polymer solution and centrifuge tube contained the 1.5 ml  $\text{CaCl}_2$  solution. Microbeads were prepared at 1500 rpm speed. Microbeads were visualized under 10X magnification with the help of inverted microscope (Zeiss). The diameter of microbeads was measured using ImageJ software after every 24 hrs. until day 6.

### **3.7.2. Degradation study of Pectin and PgA based microbeads**

Microbeads were prepared using 4 different compositions of polymers such as 9% and 10% (w/v) solution of Pectin and PgA, mixed at 1:1 and 1:3 ratio respectively. After crosslinking with  $\text{CaCl}_2$  microbeads were washed with PBS twice and again re-suspended in PBS buffer. The diameter of the microbeads was measured using ImageJ software so that it can be concluded that whether microbeads are degrading or not. This study was conducted till 14<sup>th</sup> day after microbeads were prepared.

## **3.8. Protein release study**

9% and 10% (w/v) solution of Pectin and PgA was prepared and 9% Pectin and PgA solution were mixed 1:1 and 1:3 ratio respectively and a similar proportion was also maintained for 10% solution of Pectin and PgA. The pH of these solutions was adjusted within a range of 6.5 to 7 using 2 N NaOH. BSA concentration was maintained 0.5 mg/ml for each composition of the polymer. Microbeads were prepared at 1500 rpm speed [48]. Prepared beads were washed with PBS twice and kept in PBS solution to carry out protein release study after 5 and 10 hrs of incubation at 37°C. Quantification of protein released after 5 and 10 hrs were done using Bradford reagent. 30  $\mu$ l of the sample was collected from those four experimental setups and 800 $\mu$ l of Bradford reagent was added to each set. After 5 mins of incubation O.D. was measured at 595 nm using a spectrophotometer. The quantity of protein released after 3, 6, 9 and 12 hrs was determined from the standard curve (within a range of 1 mg/ml to 0 mg/ml with an interval of 0.25) obtained for BSA protein.

## **3.9. Determination of surface topology of microbeads**

Microbeads were prepared using various composition of Pectin and PgA polymer. After centrifugation, beads were kept in  $\text{CaCl}_2$  solution for 15 minutes, so that it can crosslink

properly. Microbeads were washed with PBS and kept inside ESEM (Environmental Scanning Electron Microscope) chamber to visualize the surface topology of those microbeads. Samples were observed at 12000X magnification. Further, some microbeads were separated into two halves with the help of surgical blade and needle, to visualize the topology of the inner surface of microbeads.

### 3.10. FTIR analysis

FTIR analysis of four different samples (Pectin, Polygalacturonic acid, two different composition of microbeads) were done. Microbeads were produced using above-mentioned process, followed by washing and drying in hot air oven at 37°C respectively. Samples were in powder form and each of them was mixed with KBr (Potassium bromide). A Pellet of that mixture of sample and KBr was obtained using hydraulic press which was followed by FTIR (Fourier transform infrared spectroscopy) analysis.

### 3.11. Cell Culture

Macrophage (RAW 264.7) cell line was purchased from NCCS, Pune. DMEM, Low Glucose (Himedia) medium supplemented with 10% FBS (Himedia) and 2% of antimetabolic antibody (Himedia) was used to culture RAW 264.7 inside the incubator in a humidified 37°C, 5% CO<sub>2</sub> environment. Cell culture media was replenished after every 3 days [49].

Steps which were followed to subculture cells are described below:

- The medium from T75 flask was aspirated and cells were washed with PBS.
- Cells were detached from the bottom of the flask with the help of cell scraper.
- Cells were centrifuged at 750g for 5 mins.
- The supernatant was aspirated and cells were re-suspended in 1 ml of fresh DMEM media.
- Around 1/3<sup>rd</sup> of the cells were seeded into a new flask.
- Newly seeded Macrophages (RAW 264.7) were kept in the incubator to allow attachment overnight.
- Cells were visualized under the microscope after 24 hrs to observe whether the subculturing process had been carried out successfully.

### 3.12. Microencapsulation of Macrophages (RAW 264.7)

Microcapsules were synthesized using four different polymer composition like Pectin:PgA in 1:1 and 1:3 ratio at 9% (w/v) and 10% (w/v) concentration of Pectin as well as PgA. The polymer solution was prepared in distilled water [50]. Macrophages were encapsulated in these polysaccharide microbeads at a cell density of  $3.8 \times 10^5$  cells/ml. The polymer droplets fell into 100 mM calcium chloride solution due to centrifugal force, where the PgA crosslinked and formed microbeads. This method produced fine microbeads with a mean diameter of 327  $\mu\text{m}$ . The microbeads were kept in  $\text{CaCl}_2$  solution for 5 min to crosslink properly. This step was followed by PBS wash of microbeads twice and resuspension of beads in 5ml of complete media. The culture flasks containing encapsulated macrophages were kept inside the incubator in a humidified  $37^\circ\text{C}$ , 5%  $\text{CO}_2$  environment.

### 3.13. Determination of encapsulation efficiency

To check encapsulation efficiency cells were burst using trisodium citrate solution and heat denaturation. The total cell count before and after encapsulation was measured using trypan blue staining procedure.

### 3.14. Cell viability test using MTT

The viability of encapsulated cells was determined by MTT assay [51]. Among the enzyme-based assays, MTT assay is a most preferred technique to check a number of viable cells by determining mitochondrial dehydrogenase activities. The principal of MTT assay is based on the cleavage of the yellow-colored tetrazolium salt, 3-(4,5-dimethylthiazol-2-yl)-2,5-diphenyl tetrazolium bromide, into a blue-colored formazan because of the mitochondrial enzyme of viable cells, succinate-dehydrogenase. A solution of MTT (5 mg/mL) was prepared in PBS and sterilized by filtration technique using 0.2  $\mu\text{m}$  filter. MTT solution was added to each Petri plates, containing encapsulated cells, at 1/10th the medium volume and incubated for 4 hrs in a  $37^\circ\text{C}$ , 5%  $\text{CO}_2$  incubator. After the 4 hrs medium was removed carefully with the help of pipette to avoid disruption or removal of beads. 1ml DMSO was added to each plate and it was again incubated for 20 mins. The absorbance of the solution was measured at 595 nm with the help of

spectrophotometer [52]. Thus following protocol was followed to test the viability of cells until 9 days of encapsulation, after every 48 hrs.

### **3.15. Visualization of encapsulated cells under inverted microscope**

After 4 hrs of incubation from the addition of MTT cells were taken out from the incubator and visualized under an inverted microscope. Viable cells were stained purple and it was distinguishable under 10X, 20X and 40X magnification, using an inverted microscope (Optika).

### **3.16. Cell cytotoxicity study using LDH Assay kit**

Cell cytotoxicity was measured using LDH assay kit. RAW 264.7 cells were encapsulated in the different polymer compositions, by following above-mentioned protocol. After 24 hrs of incubation 20  $\mu$ l media from each well of encapsulated cells and control (non-encapsulated cells) was collected in triplicate manner. For positive control, cells were lysed with the help of 10X lysis buffer and after centrifugation 20  $\mu$ l supernatant was collected. Solution 1 and 2 from LDH assay kit was mixed in 4:1 ratio to make the final solution and 100  $\mu$ l was added to each well. After 15 to 20 minutes of incubation in 37°C and 5% CO<sub>2</sub> incubator, O.D. reading was measured using multi-well plate reader at 340 nm after every 30 secs until 90 secs. The whole procedure was repeated after every 48 hrs until 9 days.

### **3.17. Determination of ROS generation using NBT Assay**

Encapsulated cells and control (non-encapsulated cells) were seeded in 96 well plate in triplicate. After 24 hrs of incubation 100  $\mu$ l of media was aspirated from each well and 50  $\mu$ l of fresh media and 50  $\mu$ l of NBT working solution was added to each well [53]. In a 37°C and 5% CO<sub>2</sub> incubator, 96 well plate was kept for 2 hrs of incubation. Further, the whole solution was aspirated from each well and 140  $\mu$ l of DMSO was added after proper washing of each well. Again, it was incubated for 20 mins before collecting the O.D. reading using multi-well plate reader at 620 nm. This whole process was repeated after every 42 hrs until 9 days to conduct a time-dependent study.

### 3.18. Visualization of encapsulated cells under confocal microscope

RAW 264.7 cells were encapsulated using optimized protocol discussed above. After 5 days, a fluorescent dye (calcein) was used to stain the live cells present inside the microbeads. After aspirating whole media, 100  $\mu$ l of working solution of calcein was added. Cells were visualized under a confocal microscope at 100X magnification after 50 to 55 mins of incubation. The excitation and emission wavelengths of *calcein dye* are 495 nm and 516 nm, respectively.

### 3.19. Morphological study

The phenotype of activated macrophages can be visually distinguished based upon its morphological difference. M1 phenotype looks spherical or oval whereas M2 phenotype is more elongated [54]. In this study, macrophages were cultured on a film made of two different compositions of Pectin and PgA, 10% (w/v) 1:1 and 1:3 respectively. Cells were scraped out after five and seven days of incubation. After that macrophage were kept inside the incubator in normal tissue culture plate for ten hours to let it adhere. It was visualized using inverted microscope at 100X to check whether any morphological change has occurred in presence of anti-inflammatory environment or not. The aspect ratio of macrophages, cultured in a different environment was measured to check whether any elongation has occurred or not. Thus, the phenotype of macrophages was visually determined by studying their morphology.

## Chapter 4

# Results and Discussion

### 4.1. Optimization of diameter of PgA based microbeads

Change in rotational speed has a significant effect on change in diameter of microbeads. Moreover, the diameter of the microbeads can be controlled by changing the composition of the polymer as well as the in centrifugal force. With the increase in polymer concentration and rotational speed simultaneously, the diameter of microbeads can be decreased. In this experiment, the diameter of optimized spherical microbeads at 1900 rpm, 8% PgA (w/v) concentration is  $229.81 \pm 5.255827 \mu\text{m}$  (Figure 4.2). According to the result, the range of 1500 to 1900 rpm can be stated as the optimum speed to produce microbeads to encapsulate cells in a proper environment where chances of cell necrosis will be very less. The concentration of polymer also plays an important role in this technique, with 2% (w/v) concentration at 300 rpm speed the diameter of microbead was obtained as  $950.88 \pm 94.65064 \mu\text{m}$  (Figure 4.1) which is not suitable for cell encapsulation as it is for 8% polymer concentration at 1900 rpm. Thus, the diameter of microbeads was optimized by increasing the polymer concentration and rotation speed as depicted in (Figure 4.3).



Figure 4.1: Microbead synthesized at 300 rpm using 2% PgA (w/v) solution (at pH 5).



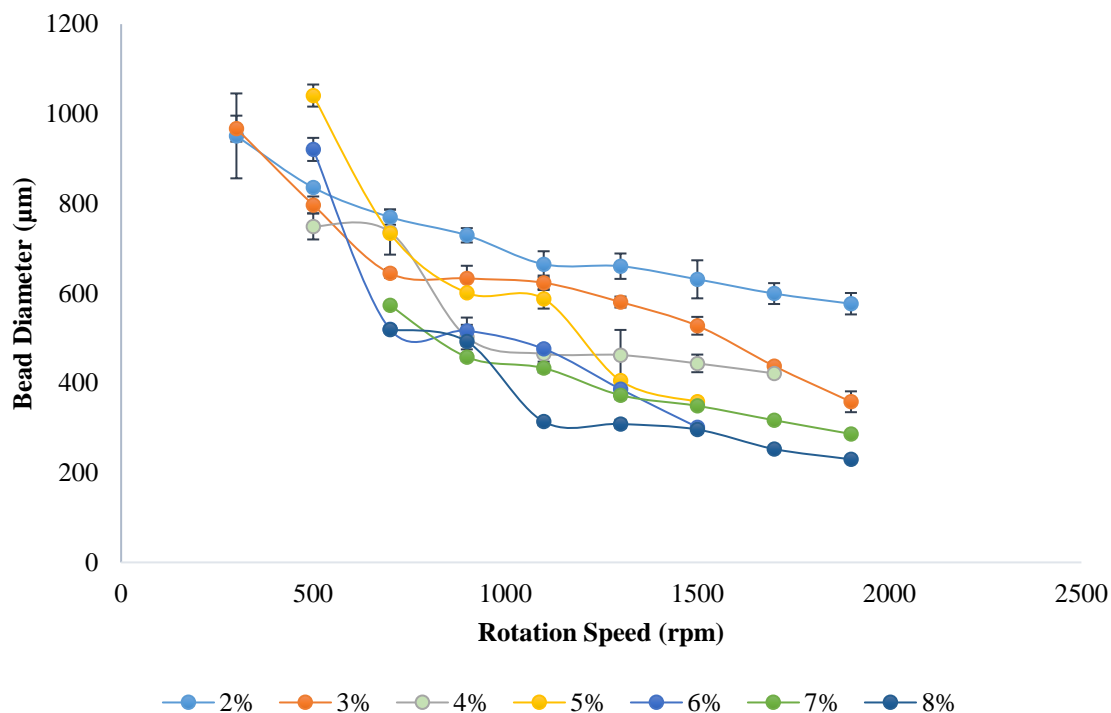


Figure 4.2: Representation of change in diameter of microbeads with respect to change in rotational speed and polymer concentration.

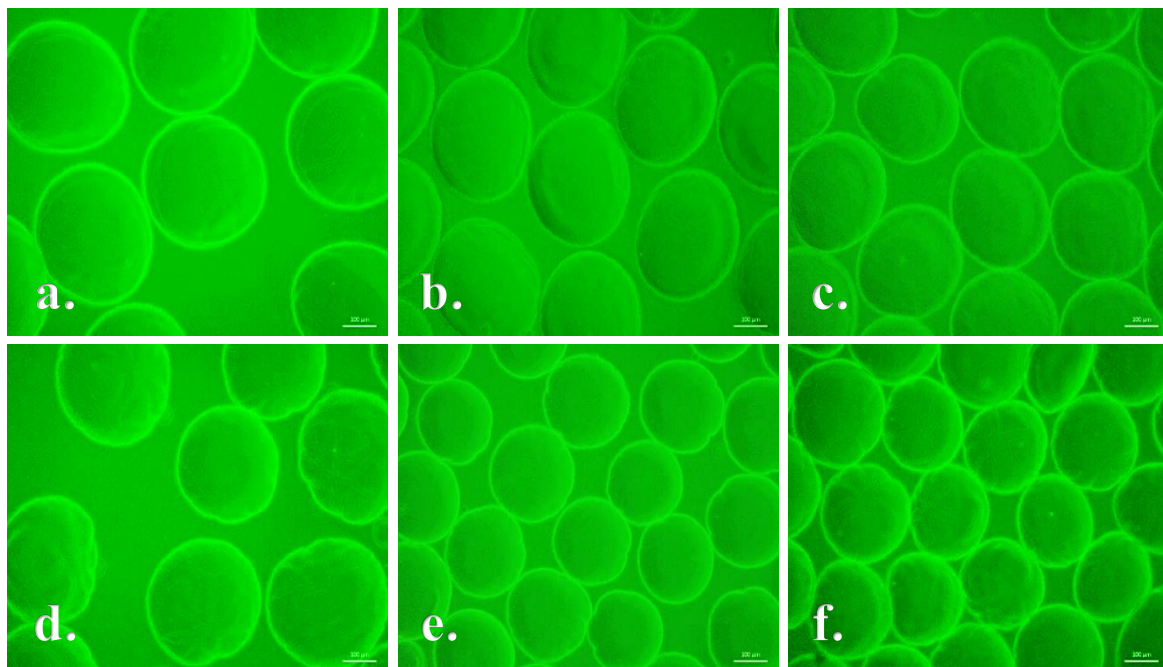


Figure 4.3: Microbeads formed at (a) 1500 rpm, (b) 1700 rpm, (c) 1900 rpm using 7% (w/v) PgA solution (at pH 5); (d) 1500 rpm, (e) 1700 rpm, (f) 1900 rpm using 8% (w/v) PgA solution (at pH 5).

## 4.2. Viscosity of Alginate and PgA polymer solution at various concentration

The viscosity of this two polymer increased with increase in its concentration. But viscosity of PgA at lower concentration (2%, 3%, 4%, 5% w/v) was so low that it was beyond the detection level of the viscometer. For PgA viscosity of the solution increased with increase in pH up to 5. But beyond that level viscosity dropped down tremendously with an increase in pH value which was beyond detection level of the viscometer. If we compare the viscosity of the Alginate with PgA it can be stated that Alginate solution at lower concentration (2% w/v) is much viscous than PgA solution at that concentration. The result is depicted below (Figure 4.4).

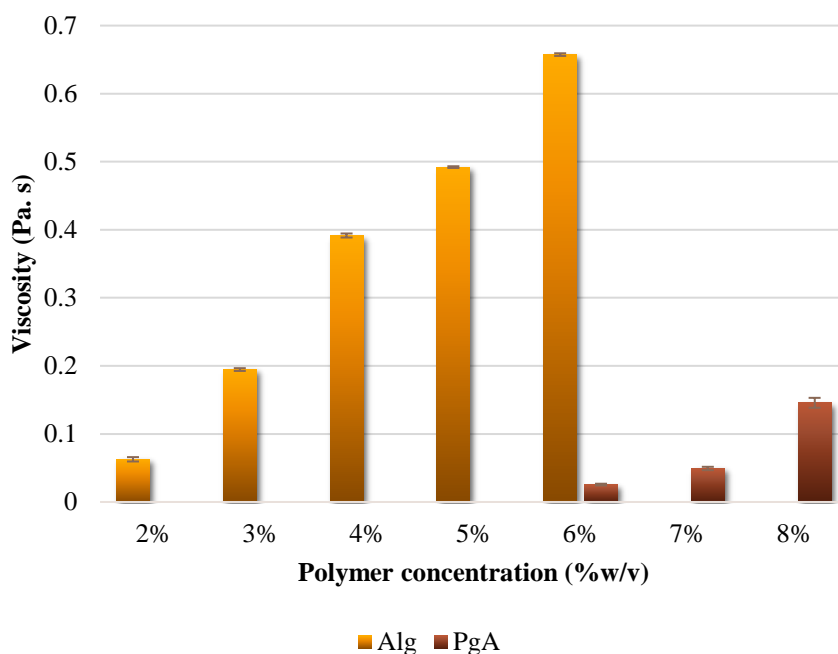


Figure 4.4: Representation of change in viscosity with the change in concentration of polymers including Alginate and PgA.

## 4.3. Hemocompatibility of PgA based microbeads

The *in vitro* hemolysis assay was carried out to evaluate the hemocompatibility of microbeads synthesized using a different concentration of PgA (Figure 4.5). Hemolysis Percentage was much less than 5%. Hence, it can be stated that both the polymers are hemocompatible.

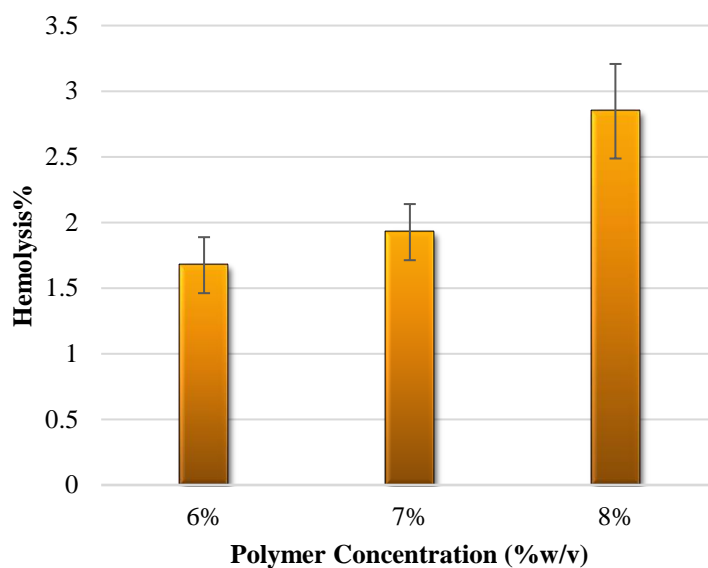


Figure 4.5: Hemolysis Percentage at different concentration of PgA solution.

#### 4.4. Degradation study of PgA based microbeads

7% and 8 % (w/v) concentration of PgA was used to synthesize microbeads at 1500 rpm speed and it was kept in PBS solution for 6 days. A minor reduction in diameter of microbeads occurred from day 0 to day 6, as depicted below (Figure 4.6). The diameter of microbeads produced using 7% and 8% (w/v) PgA solution, decreased approximately 5.44 and 2.66  $\mu\text{m}$  respectively, which does not interpret any significant change.

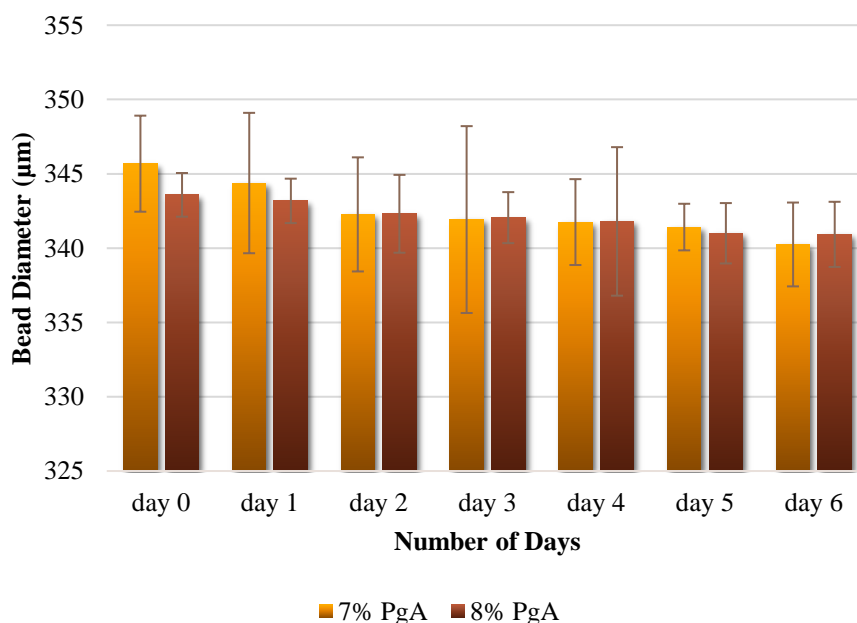


Figure 4.6: Representation of change in the diameter of microbeads with respect to time.

## 4.5. PgA based microbeads preparation at pH 7

As discussed before at pH 7 the viscosity of PgA solution dropped down tremendously. Microbeads formed using that polymer solution got distorted because of very low viscosity (Figure 4.7). Hence, cell encapsulation is not possible in this condition. Because animal cells need to be maintained at a pH range of 7.2 to 7.4. However, this microbead system using PgA can be used in drug loading purpose where pH 5 is suitable.

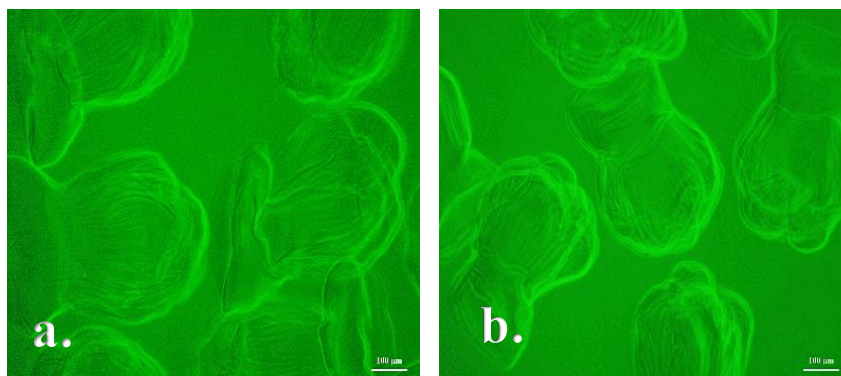


Figure 4.7: Microbeads produced at 1500 rpm using (a) 7% and (b) 8% (w/v) Polygalacturonic acid (at pH 7).

## 4.6. Optimization of diameter of Pectin and PgA based microbeads

Change in rotational speed has a significant effect on change in diameter of microbeads. Moreover, the diameter of the microbeads can be controlled by changing the composition of the polymer as well as the centrifugal force. With the increase in polymer concentration and rotational speed simultaneously, the diameter of microbeads can be decreased. But at a very high rotational speed like 1900 rpm the shape of the microbeads became distorted (Figure 4.9). In this experiment, the diameter of optimized spherical microbeads at 1500 rpm varies from 308 to 346  $\mu\text{m}$  (Figure 4.8). At 1700 rpm the diameter of microbeads ranges from 286 to 206  $\mu\text{m}$  (Figure 4.8). But at 1700 rpm microbeads were not able to maintain its spherical shape properly. Hence, 1500 rpm can be stated as the optimum speed to produce microbeads to encapsulate cells in a proper environment where chances of cell necrosis will be very low due to unavailability of nutrition and oxygen.

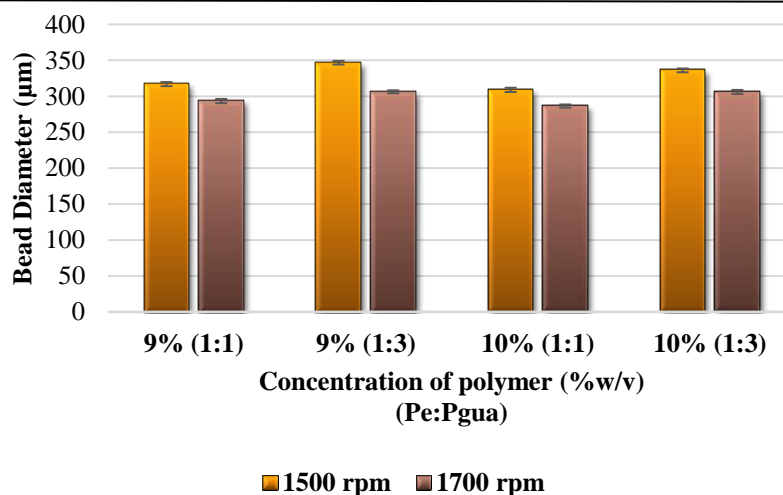


Figure 4.8: Representation of change in diameter of microbeads with respect to change in rotational speed and polymer composition.

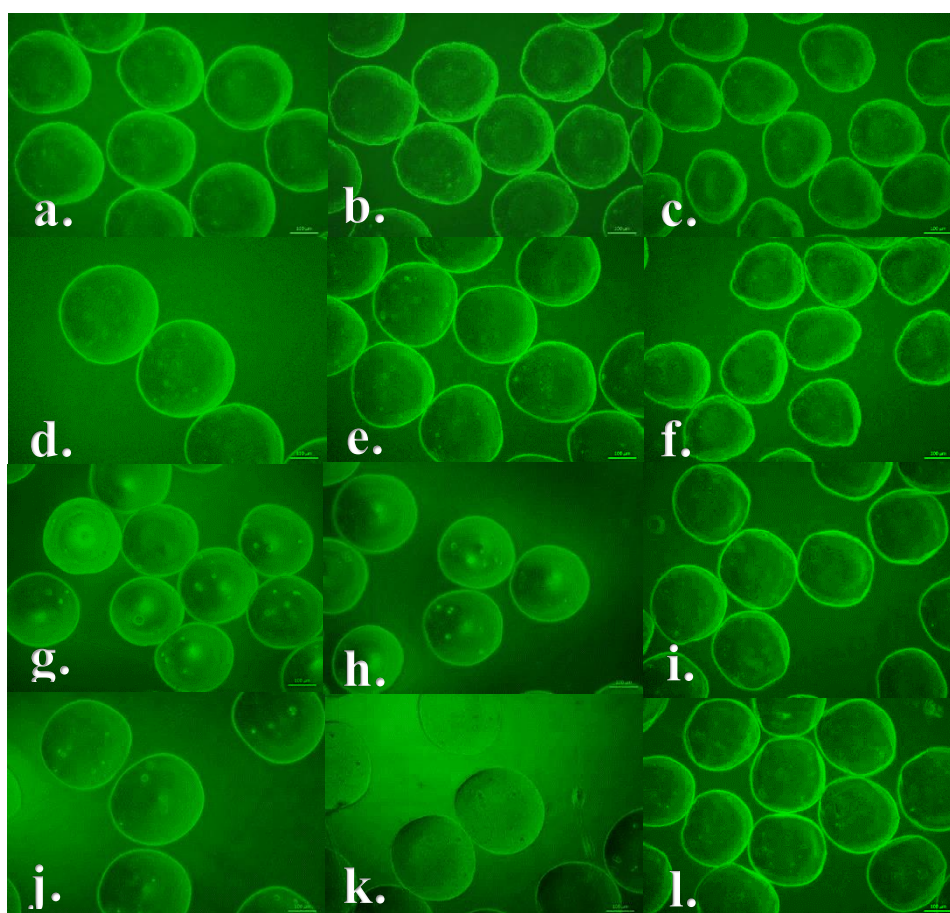


Figure 4.9: Microbeads produced at (a) 1500 rpm, (b) 1700 rpm, (c) 1900 rpm using polymer composition 9% (w/v) (Pectin:PgA at 1:1 ratio); (d) 1500 rpm, (e) 1700 rpm, (f) 1900 rpm using polymer composition 9% (w/v) (Pectin:PgA at 1:3 ratio); (g) 1500 rpm, (h) 1700 rpm, (i) 1900 rpm using polymer composition 10% (w/v) (Pectin:PgA at 1:1 ratio); (j) 1500 rpm, (k) 1700 rpm, (l) 1900 rpm using polymer composition 10% (w/v) (Pectin:PgA at 1:3 ratio).

#### 4.7. Viscosity measurement of various composition of Pectin and PgA polymer solution

Viscosity increased with increase in polymer concentration, especially when the proportion of PgA was more than Pectin, as shown below (Figure 4.10). By analyzing the viscosity and diameter of microbeads formed at 1500 rpm using the same composition of the polymer, it can be stated that diameter of microbeads reduced with an increase in viscosity of the solution.

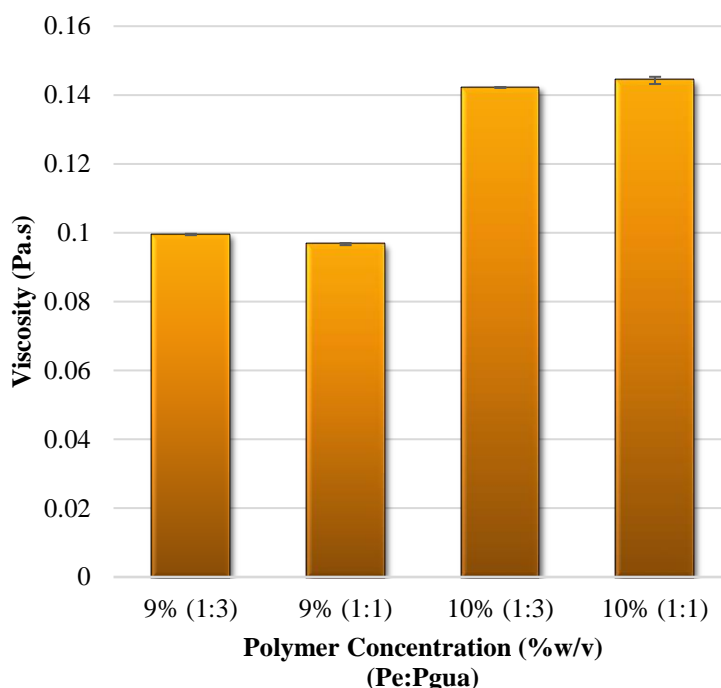


Figure 4.10: Representation of change in viscosity with respect to polymer composition.

#### 4.8. Hemocompatibility of Pectin and PgA based microbeads

The *in vitro* hemolysis assay was carried out to evaluate the hemocompatibility of microbeads synthesized using different composition of Pectin and PgA (Figure 4.11). Hemolysis Percentage for each composition was much less than 5%. Hence, it can be stated that both the polymers are highly hemocompatible and suitable for application in chronic wound healing.

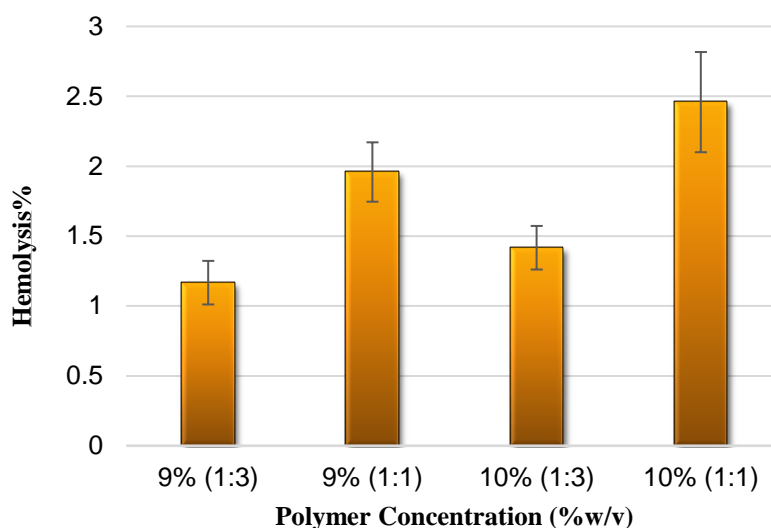


Figure 4.11: Hemolysis Percentage of different composition of Pectin and PgA based microbeads.

#### 4.9. Production of microbeads using three different polysaccharide-based polymers at 1500 rpm speed

Microbeads were synthesized using different types of polysaccharide polymer composition including Alginate, PgA and Pectin+PgA. The determined diameter of the microbeads depicts that microbeads composed of Alginate have smallest diameter, followed by Pectin+PgA and PgA respectively (Figure 4.12). This is because Alginate has higher viscosity among those three polymer solutions.

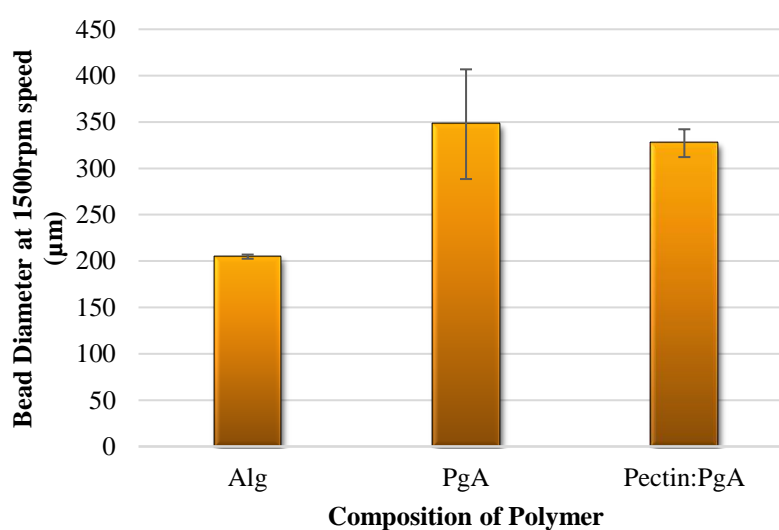


Figure 4.12: Microbead production using three different polysaccharide based polymers.



### 4.10. Degradation study of PgA based microbeads

Initially, the diameter of microbeads was almost similar. After fourteen days, a minor decrease in diameter occurred for each of four samples. The microbead diameter of the sample with polymer composition 10% (w/v) (Pectin:PgA at 1:1 ratio), decreased the most and it was approximately decreased by 46  $\mu\text{m}$ . But the average decrease in diameter size, at the end of the experiment, was not more than 35 $\mu\text{m}$  (Figure 4.13). Hence, it can be concluded that these microbeads would sustain till the chronic wounds get healed.

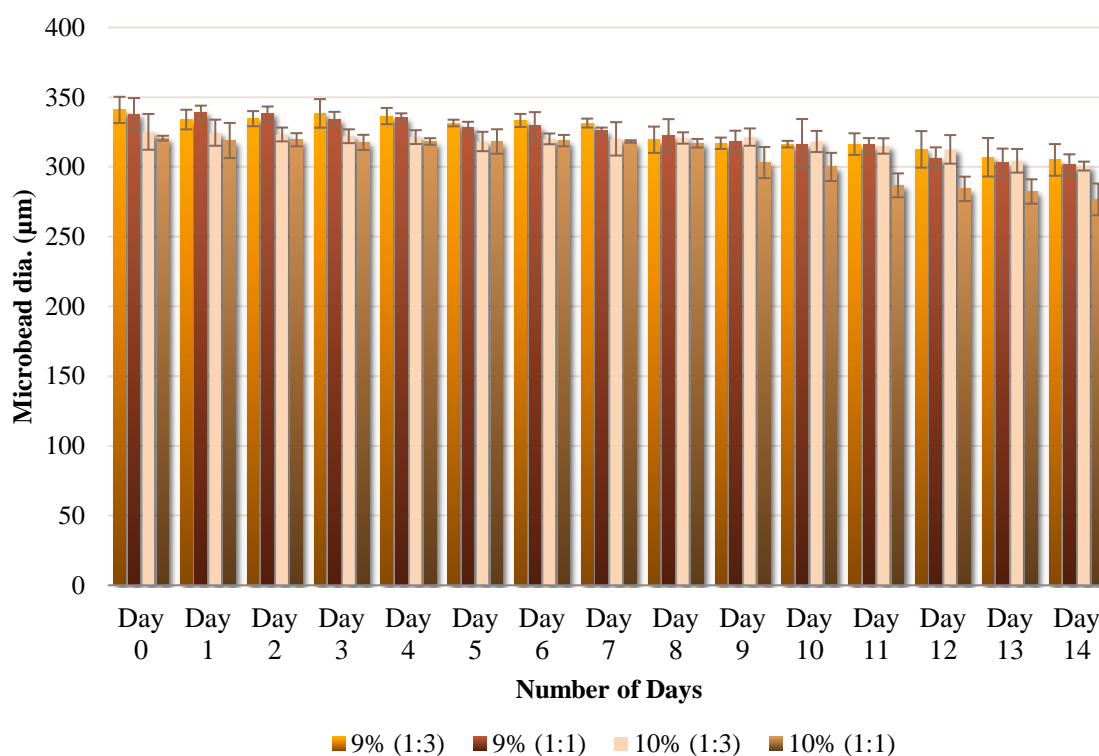


Figure 4.13: Representation of decrease in diameter of microbeads with respect to time.

### 4.11. Protein release study

Bovine serum albumin (BSA) encapsulated microbeads were incubated at 37°C to determine the protein release after 5 and 10 hrs. Experimental results obtained from Bradford assay depicted time-dependent study of release of encapsulated protein (Figure 4.14). The highest degree of protein release was obtained for the 10% polymer concentration (with Pectin:PgA = 1:1) as depicted below (Figure 4.14). This might have happened because microbeads composed of 10% (1:1) polymer has lowest microbead



diameter among those four samples. Since, molecular weight as well as a number of amino acids of BSA (66.5kDa, 583 amino acids) is higher than IL-10 (20.52kDa, 178 amino acids), it can be stated that IL-10 will be secreted out from these microbeads. Hence, these microbeads can be used for the treatment of chronic wounds after checking its anti-inflammatory properties.

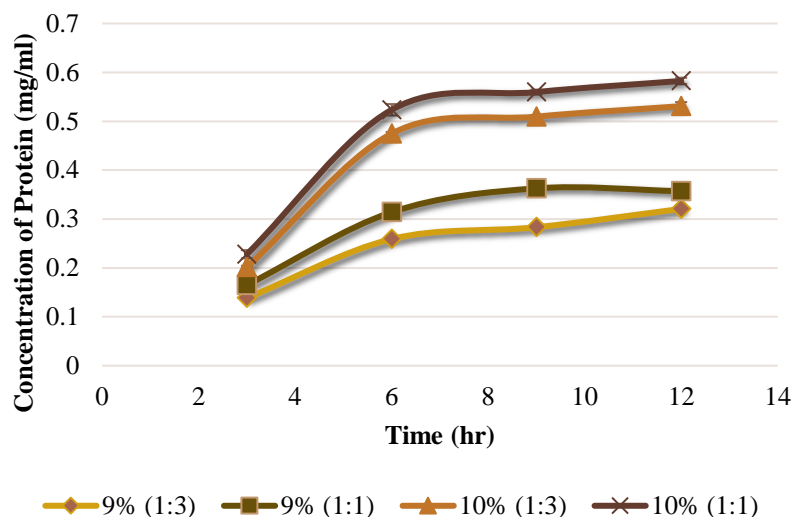


Figure 4.14: Representation of protein release study.

## 4.12. FTIR Analysis

For pure Pectin sample six significant Peaks were observed at  $2932\text{ cm}^{-1}$  (C-H, stretching),  $1742\text{ cm}^{-1}$  (C=O, stretching),  $1632\text{ cm}^{-1}$  (C-H, bending),  $1443\text{ cm}^{-1}$  (C-H, bending),  $1347\text{ cm}^{-1}$  (C-H, bending),  $1066\text{ cm}^{-1}$  (C-O, stretching). Six significant Peaks were also observed for pure PgA sample, which includes  $2932\text{ cm}^{-1}$  (C-H, stretching),  $1742\text{ cm}^{-1}$  (C=O, stretching),  $1630\text{ cm}^{-1}$  (C-H, bending),  $1412\text{ cm}^{-1}$  (O-H, bending),  $1334\text{ cm}^{-1}$  (C-H, bending),  $1096\text{ cm}^{-1}$  (C-O, stretching). Whereas in case of microbeads composed of 10% (w/v) (Pectin:PgA at 1:1 ratio) five different Peaks were most significant like  $1632\text{ cm}^{-1}$  (C-H, bending),  $1424\text{ cm}^{-1}$  (O-H, bending),  $1106\text{ cm}^{-1}$  (C-O, stretching) and  $1026\text{ cm}^{-1}$  (C-O, stretching). Further, six significant Peaks were detected for microbeads composed of 10% (w/v) (Pectin:PgA at 1:3 ratio) like  $2950\text{ cm}^{-1}$  (C-H, stretching),  $1632\text{ cm}^{-1}$  (C-H, bending),  $1456\text{ cm}^{-1}$  (C-H, bending),  $1136\text{ cm}^{-1}$  (C-O, stretching) and  $1057\text{ cm}^{-1}$  (C-O, stretching). The breaking of the dimer is consistent for both the samples of microbeads. This might have happened during crosslinking with  $\text{CaCl}_2$ .

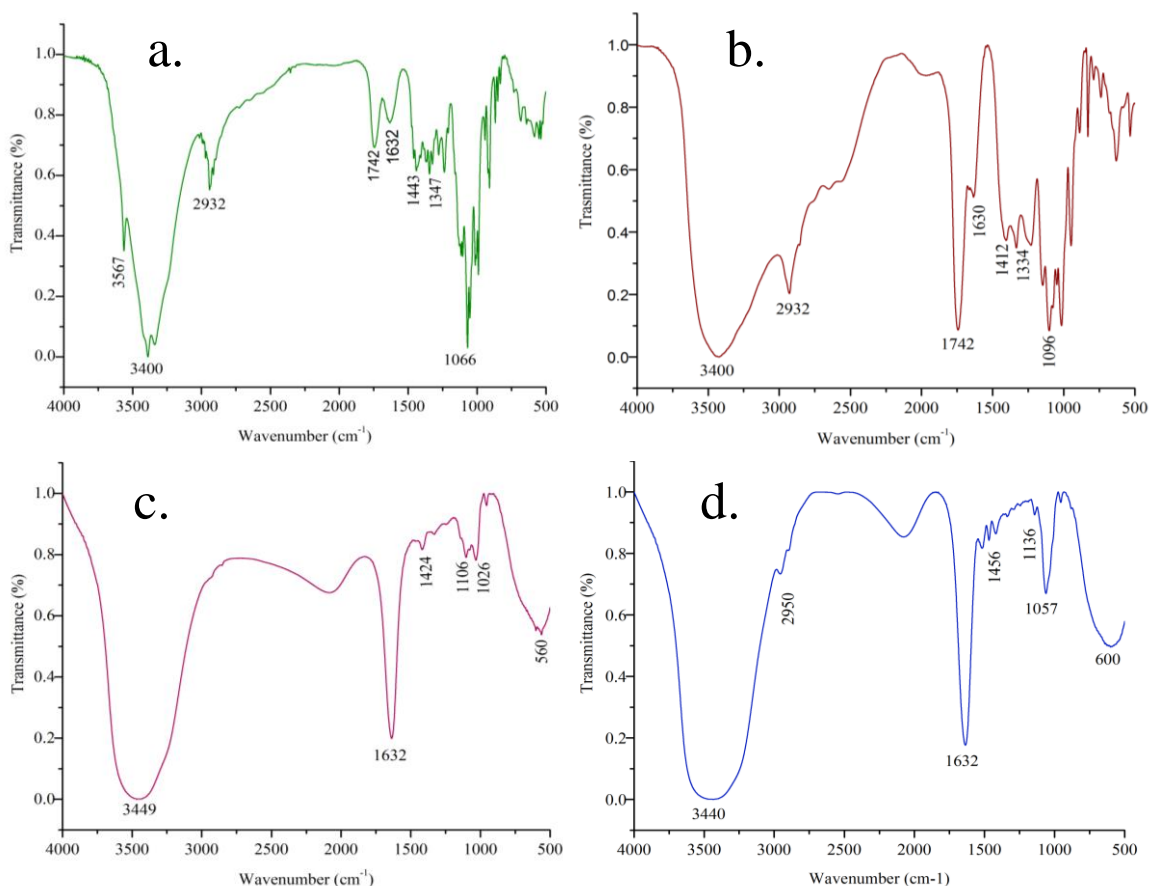


Figure 4.15: Representation of FTIR analysis: (a) Pectin; (b)PgA; (c) Pectin:PgA at 1:1 ratio, 10% (w/v) and (d) Pectin:PgA at 1:3 ratio, 10% (w/v)

### 4.13. Surface topology of Microbeads

Surface topology of microbeads was observed using ESEM (Environmental Scanning Electron Microscope). With the change in the composition of the polymer, surface topology of microbeads was also changed. Visually, the surface of the composition, Pectin:PgA at 1:3 seemed to be more rigid than at 1:1 (Figure 4.17). The inner portion of microbead was also visualized at 2000X magnification (Figure 4.16).

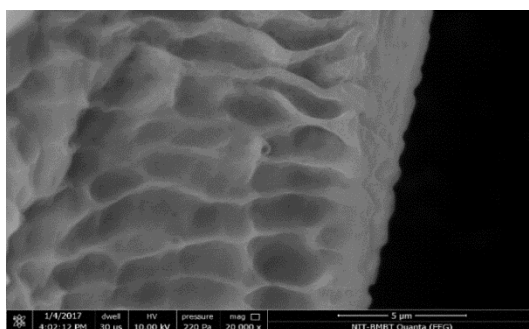


Figure 4.16: Inner structure of Microbead.

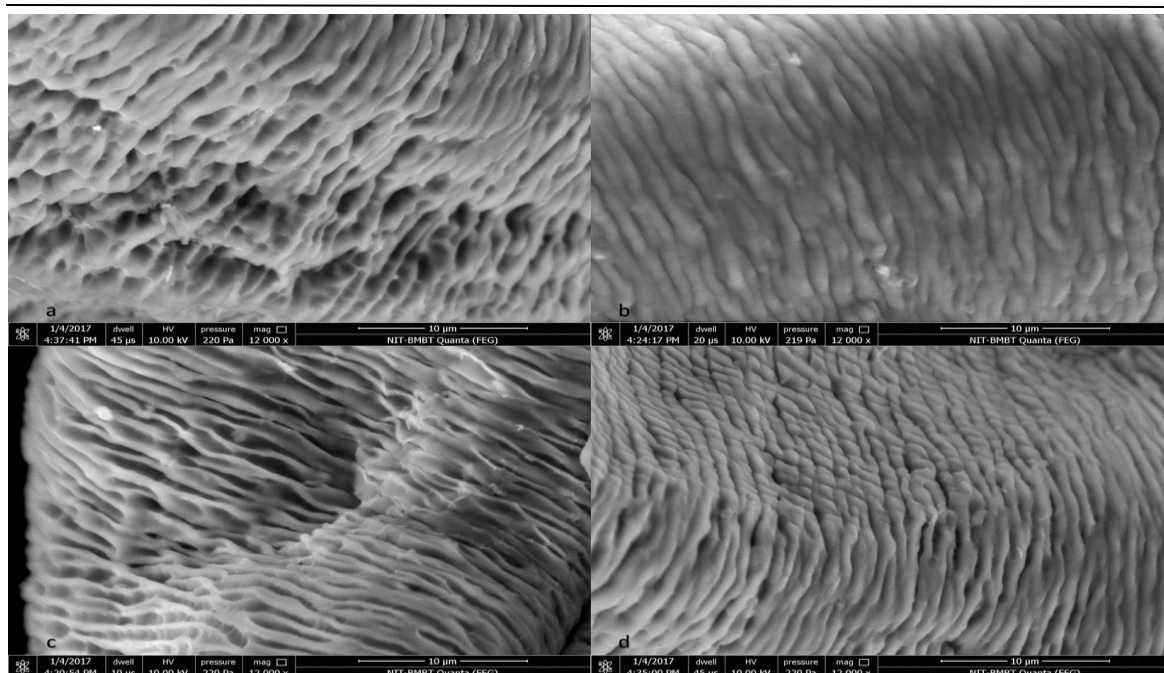


Figure 4.17: Surface topology of Microbeads with different polymer concentration, (a) 9% (w/v) ( Pectin:PgA at 1:1 ratio), (b) 9% (w/v) ( Pectin:PgA at 1:3 ratio), (c) 10% (w/v) (Pectin:PgA at 1:1 ratio), (d) 9% (w/v) ( Pectin:PgA at 1:3 ratio).

#### 4.14. Determination of encapsulation efficiency

The encapsulation efficiency was measured using Trypan Blue staining method. Total no. of cells before encapsulation in each polymer composition was  $2.15 \times 10^5$  cells/ml, and calculated total no. of cells after encapsulation was  $1.33 \times 10^5$  cells/ml,  $1.28 \times 10^5$  cells/ml for 10% (w/v) (Pe:PgA at 1:1 ratio) and 10% (w/v) (Pectin:PgA at 1:3 ratio) respectively (Figure 4.18). Hence Percentage encapsulation efficiency for 10% (w/v) (Pectin:PgA at 1:1 ratio) and 10%(w/v) (Pe:PgA at 1:3 ratio) composition are 61.86% and 59.53% respectively.

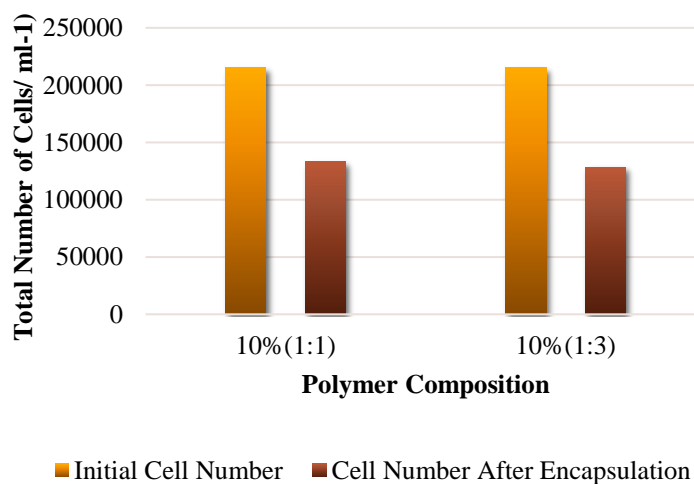


Figure 4.18: Representation of encapsulation efficiency.

### 4.15. Encapsulation of macrophages

Viable encapsulated cells were observed under a microscope. Only viable cells were stained during MTT assay and those were distinguishable under 10X, and 40X magnification (Figure 4.19).  $1 \times 10^6$  cells/ml were encapsulated, using 1ml of the polymer. Encapsulated cells were visualized, under the microscope after one, three, five, seven and nine days of incubation in a humidified 37°C, 5% CO<sub>2</sub> environment.

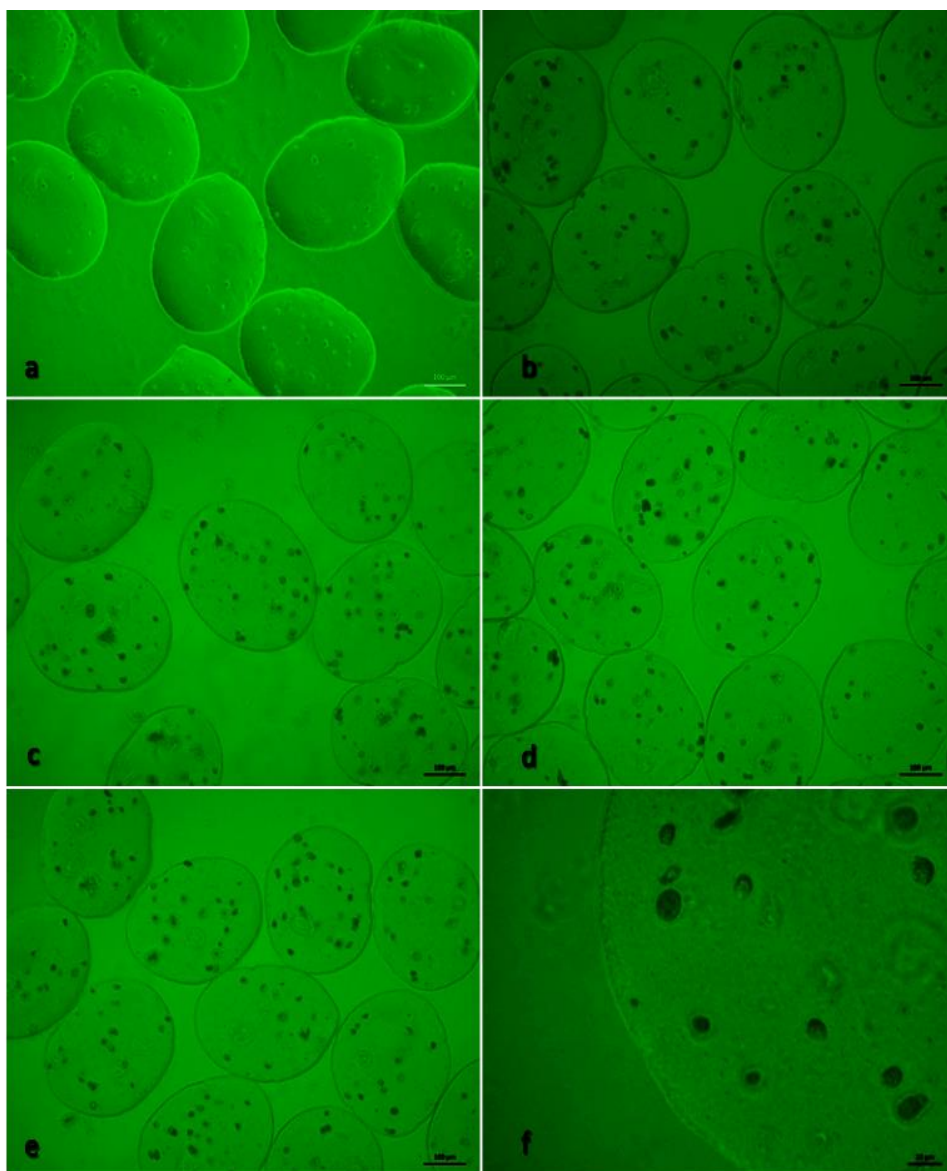


Figure 4.19: Visualization of cell proliferation inside microbeads, under inverted microscope at 100X magnification (a) Day 1, (b) Day 3, (c) Day 5, (d) Day 7, (e) Day 9; and 400X magnification (f) Day9.

### 4.16. Viability of encapsulated cells: MTT assay

After 24 hrs, observed cell viability was more in the case of control (non-encapsulated cells). But in the case of encapsulated cells amount of viable cells is much lower. This might have happened because encapsulation efficiency is not 100%. Hence, many cells might have washed away during the encapsulation process. Further, 96 hrs later, MTT assay results depict that viability of cells were increased with respect to decreasing in diameter of the microbeads. Diameter of microbeads with polymer composition 10% (w/v) (Pe:PgA at 1:1 ratio) was lesser than microbeads formed with polymer composition 9% (w/v) (Pe:PgA at 1:3 ratio) and 10% (w/v) (Pectin:PgA at 1:3 ratio). Hence, the highest number of viable cells were observed for microbead diameter  $308.8 \pm 2.962045 \mu\text{m}$ . Thus cell viability was measured with the help of MTT assay on first, third, fifth, seventh and ninth day (Figure 4.20).

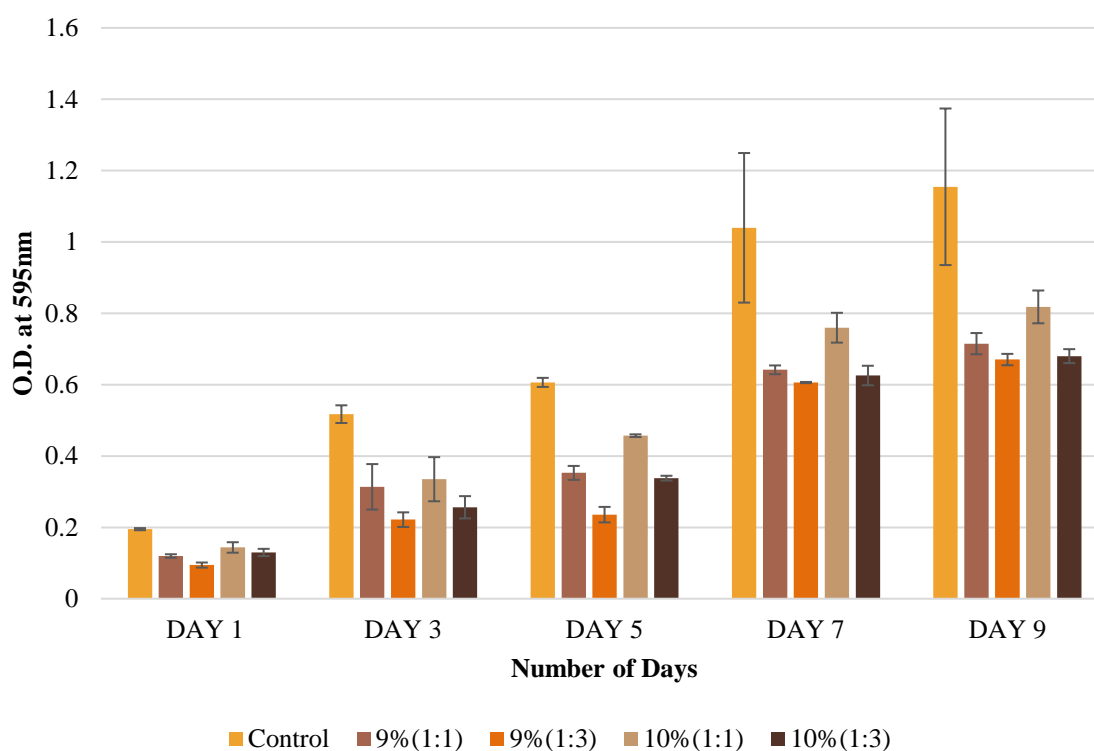


Figure 4.20: Representation of effect on cell viability due to encapsulation.

Percentage cell viability differed with respect to change in the polymer composition. The highest percentage of viability was observed in the case of 10% (w/v) Pectin:PgA= 1:1, which ranges in between seventy to seventy-five percent. This was followed by 9% (w/v) Pectin:PgA= 1:1, 10% (w/v) Pectin:PgA= 1:3, and 9% (w/v) Pectin:PgA= 1:3.

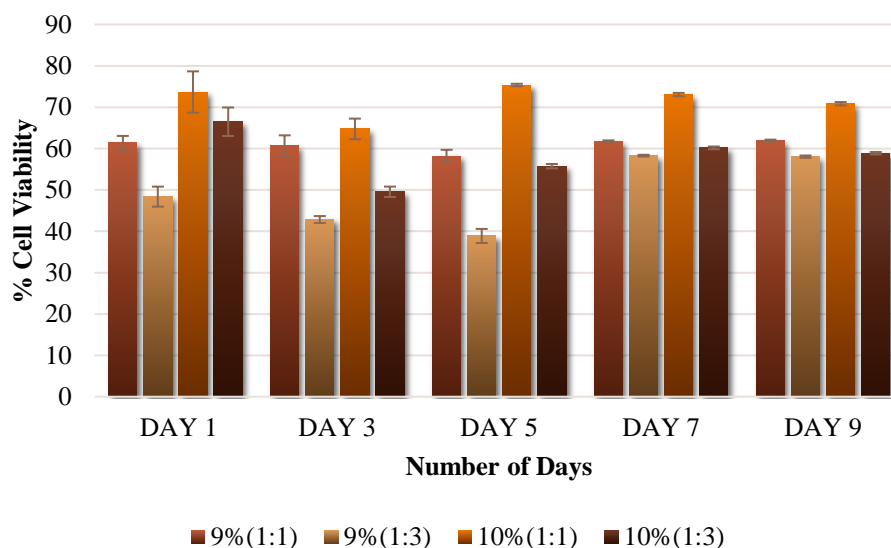


Figure 4.21: Representation of percentage cell viability.

#### 4.17. Measurement of cell cytotoxicity: LDH assay

Two major forms of cell death observed in normal condition as well as in disease pathologies are necrosis and apoptosis. Permeabilization of the plasma membrane is the hallmark of necrotic cells. Moreover, necrosis is caused due to swelling and rupture of intracellular organelles and this leads to the breakdown of the entire plasma membrane. Hence, intracellular components come out into extracellular space because of impaired plasma membrane and cause inflammatory responses. Necrosis of cells can be measured with the help of cytotoxicity assays. These assays could be principally divided into two categories: one is based on uptake of Propidium iodide (DNA binding dye), another is based on leakage of intracellular components to the extracellular milieu through the damaged plasma membrane. Moreover, measurement of the amount of released lactate dehydrogenase (LDH) helps us to quantify this particular event. The result (Figure 4.21) shows that cytotoxicity level for each composition of the polymer is not at all unhealthy for cells. Moreover, the condition is not unpleasant if LDH activity is less than 100 IU/L. Hence, the system is fine for further consideration.

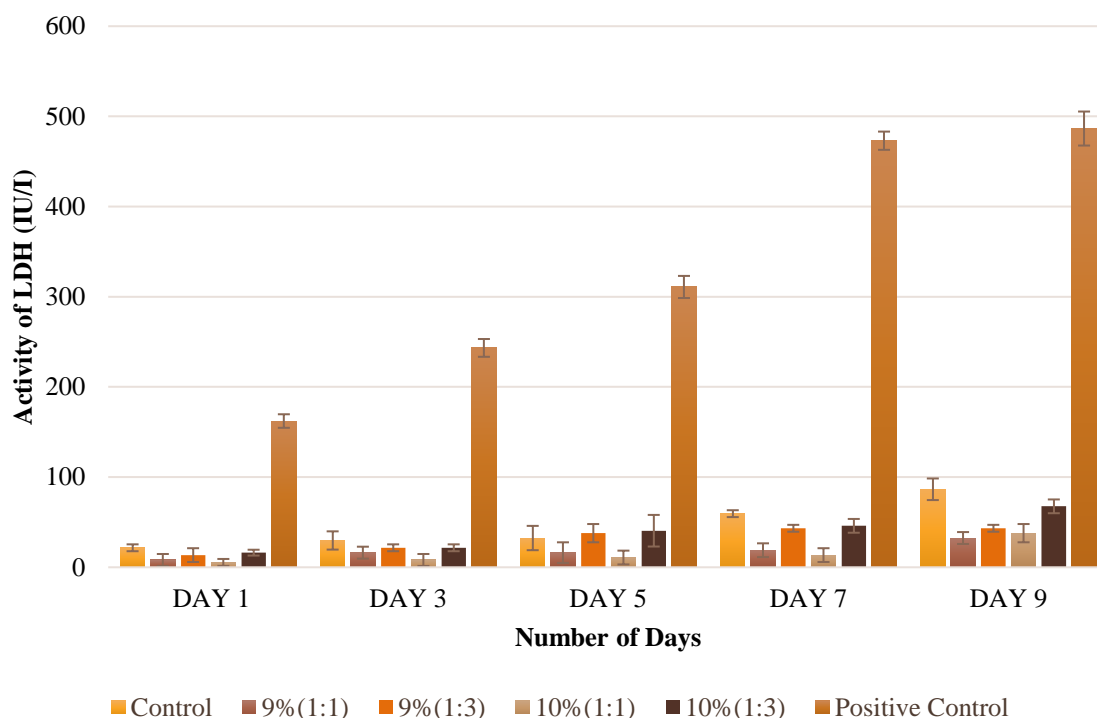


Figure 4.22: Representation of cell cytotoxicity level.

#### 4.18. Superoxide assay: NBT reduction

The over-generation of ROS leads to Permanent cell damage by evoking an intracellular state of oxidative stress. But indirectly it shows the effect of NADPH oxidase. In this assay intense color change means more NADPH oxidase activity of macrophages. Hence, it can be used to determine the presence of activated macrophages. The result (Figure 4.22) depicts the change of polymer composition has an effect on macrophage activation. Since LDH assay results concluded that the microbead system has provide healthy environment to the cells, it can be concluded that in this system amount of generated ROS will not have any unpleasant effect on cells.



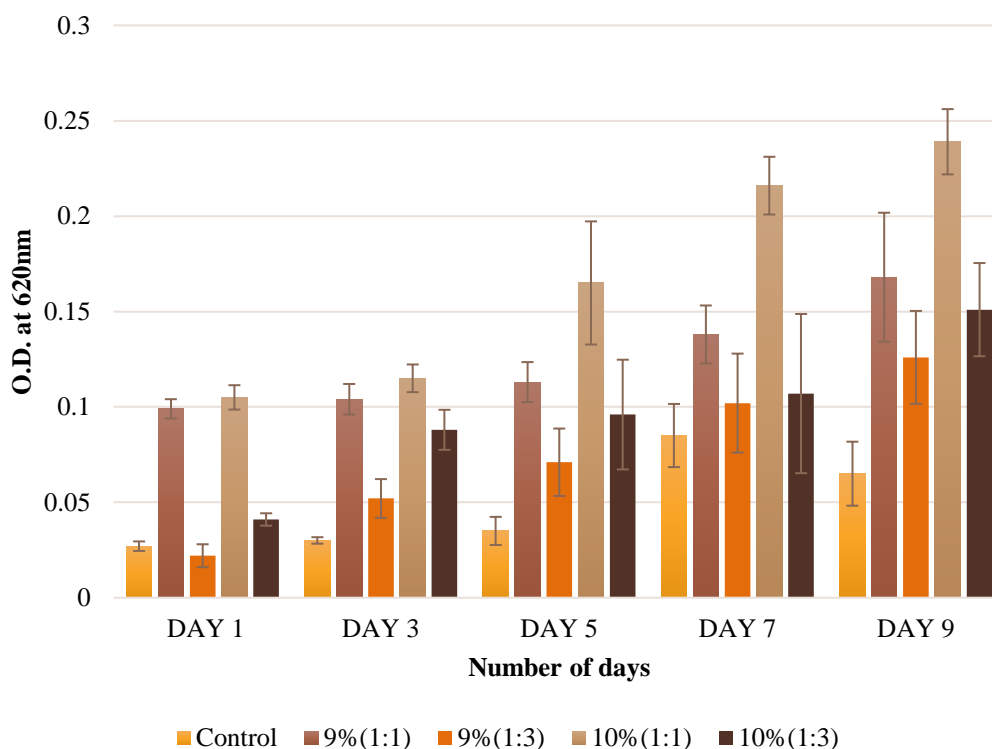


Figure 4.23: Representation of activation of macrophages with respect to polymer composition.

#### 4.19. Visualization of alive cells inside microbeads

The calcein assay is based on the principle of intracellular esterase activity in alive cells which causes the conversion of the cell permeant non-fluorescent calcein AM dye to the fluorescent dye. Macrophages were encapsulated in four different compositions of Pectin and PgA. Encapsulated macrophages were visualized under the confocal microscope after five days of incubation. The average no. of cells per microbead is approximately thirty (Figure 4.23).

Table 4.1: Tabulation of an approximate number of alive cells in each microbead.

Polymer composition	Number of cells in each microbead
9%(w/v) (Pectin:PgA at 1:1 ratio)	$28 \pm 6$
9%(w/v) (Pectin:PgA at 1:3 ratio)	$27 \pm 6$
10%(w/v) (Pectin:PgA at 1:1 ratio)	$29 \pm 5$
10%(w/v) (Pectin:PgA at 1:3 ratio)	$27 \pm 5$



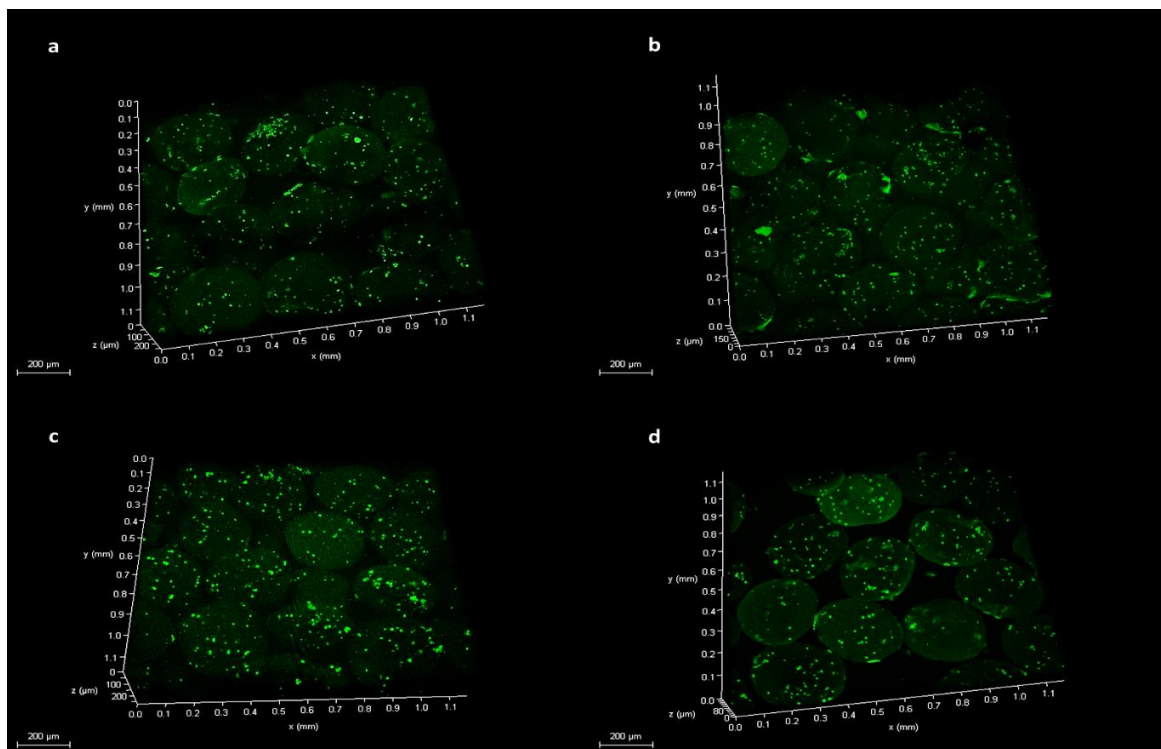


Figure 4.24: Visualization of encapsulated macrophages in different composition of polymer, (a) 9% (w/v) (Pectin:PgA at 1:1 ratio), (b) 9% (w/v) (Pectin:PgA at 1:3 ratio), (c) 10% (w/v) (Pectin:PgA at 1:1 ratio), (d) 10% (w/v) (Pectin:PgA at 1:3 ratio) under confocal microscope.

## 4.20. Morphological study

Macrophages were cultured on the top of the films, made of the different composition of Pectin and PGA. After five and seven days of incubation, cells were observed under an inverted microscope to study the morphological changes. For control sample where cells were cultured in normal tissue culture plate, macrophages remained un-activated (Figure 4.24). Whereas macrophages cultured on Pectin and PgA based films elongated after five days of incubation and they further elongated until the seventh day (Figure 4.24). The aspect ratio was also determined and it was in a range of 1.5 to 2 for control and 4 to 6, 4.5 to 7.5 for experimental samples after five and seven days respectively (Figure 4.25). This result depicts that un-activated macrophages polarize into M2 phenotype in presence of Pectin and PgA.

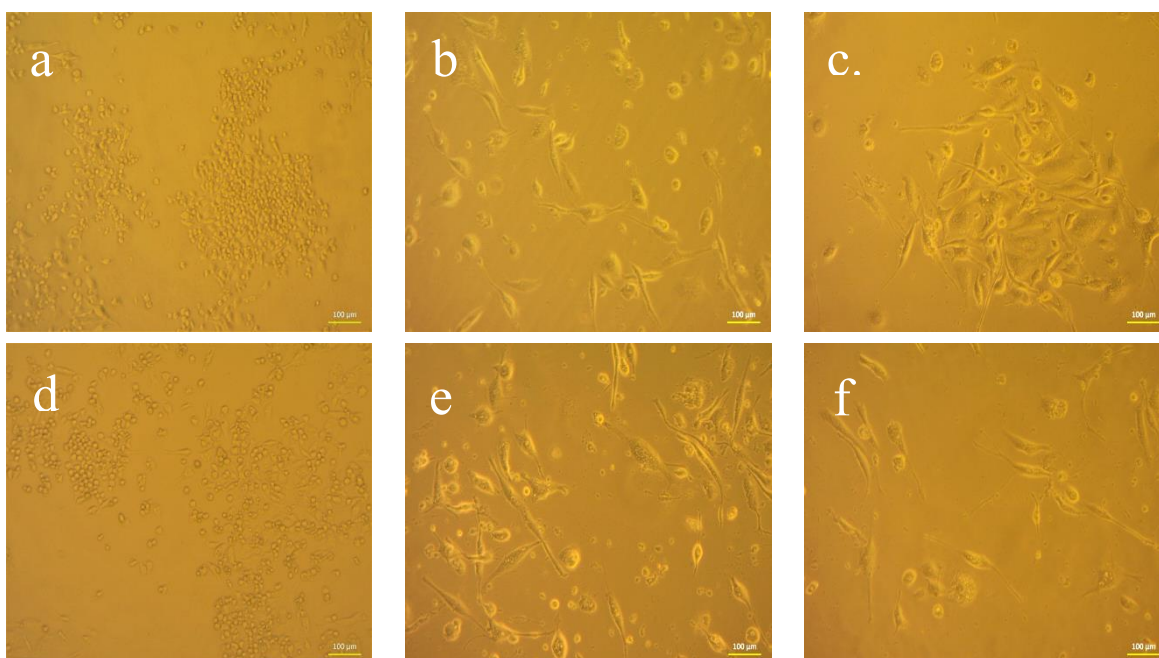


Figure 4.25: Effect of anti-inflammatory environment on polarization of macrophages: Observation on day 5: (a) control, (b) cultured on 10% (w/v)( Pectin:PgA at 1:1 ratio), (c) 10% (w/v)( Pectin:PgA at 1:3 ratio); observation on day 7: (d) control, (e) culture on 10% (w/v)( Pectin:PgA at 1:1 ratio), (f) 10% (w/v)( Pectin:PgA at 1:3 ratio).

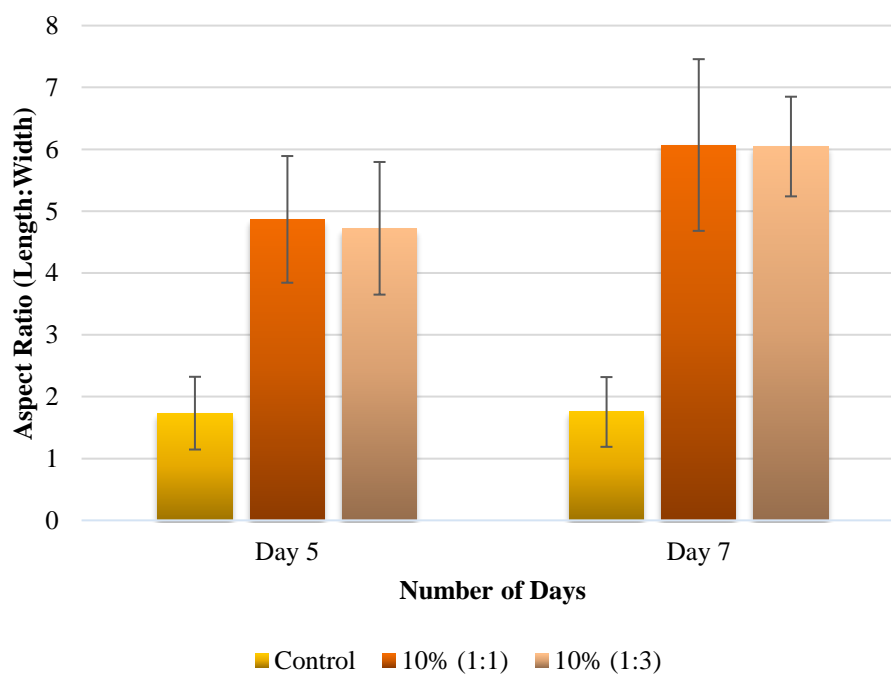


Figure 4.26: Representation of macrophage elongation with respect to polymer composition and time.

## Chapter 5

# Conclusion

Complete wound healing requires a balance in between pro-inflammatory and anti-inflammatory phase to repair the wound bed within the stipulated time. Hence, proper polarization of macrophages of required phenotype, according to the stage of wound healing is very important. Macrophages can be polarized from un-activated state to activated M1 or M2 phenotype in presence of external stimuli. The M1 phenotype can be generated by inducing unactivated macrophages in presence of microbial stimuli (e.g., Lipopolysaccharides), pro-inflammatory cytokines (e.g., IFN $\gamma$ , TNF), and growth factors (e.g., GM-CSF). On the other hand, the polarization of macrophages to M2 phenotype occurs in presence of anti-inflammatory cytokines (e.g., IL 10, IL-4, IL-13), and hormones (e.g., secosteroid, glucocorticoid). Therefore, a proper understanding of molecular mechanisms and micro-environmental stimuli, involved in macrophage polarization would permit us to manipulate as well as to regulate those specific physiological processes, which are involved in chronic wound healing.

The introduction of M2 macrophages at the site of chronic wound seems an effective strategy to treat chronic wounds since they play a key role in modulating inflammatory responses. Major challenges in implementing such strategy are prevention of macrophages from washing out from the site of injury, avoiding any immunological reaction due to the incorporation of foreign cells, and sustenance of macrophage phenotype over the period of healing. Hence, microbead-based technology is an effective strategy for immunomodulation of chronic wounds and its early resolution.

Pectin and PgA based microbeads can be used to encapsulate cells. The centrifuge tube-syringe setup can be used produce microbeads, having the desired diameter for the purpose of cell encapsulation. This is a very cost effective method where centrifugal force plays an important role in the production of microbeads. The rotational speed of 1500 rpm can be stated as an optimized parameter to synthesize microbeads having a diameter less than 350  $\mu\text{m}$ .

Cells maintained proper viability in an efficient manner within this range of microbead diameter. Since, very few cell death occurs in this environment, it can be inferred that

microbeads provided proper availability of nutrition and oxygen supply. Pectin and PgA based microbeads do not hinder cell proliferation and this macrophage-microbead system remained stable for more than a week.

Pectin and PgA are found to be highly hemocompatible in nature. These polysaccharide based polymers do not have any cytotoxic effect on the cells when used for the purpose of encapsulation. Further, encapsulation of macrophages in Pectin and PgA based microbeads might help the un-activated macrophages to polarize in M2 phenotype due to anti-inflammatory property of these polysaccharides. Thus, chronic wounds might get healed within lesser time span by following proposed strategy.

# References

- [1] Mustoe, Thomas A., Kristina O'shaughnessy, and Oliver Kloeters. "Chronic wound pathogenesis and current treatment strategies: a unifying hypothesis." *Plastic and reconstructive surgery* 117, no. 7S (2006): 35S-41S.
- [2] Menke, Nathan B., Kevin R. Ward, Tarynn M. Witten, Danail G. Bonchev, and Robert F. Diegelmann. "Impaired wound healing." *Clinics in dermatology* 25, no. 1 (2007): 19-25.
- [3] Robson, Martin C., and Adrian Barbul. "Guidelines for the best care of chronic wounds." *Wound repair and regeneration* 14, no. 6 (2006): 647-648.
- [4] Gilmore, M. A. "Phases of wound healing." *Dimensions in oncology nursing: journal of the Division of Nursing* 5, no. 3 (1990): 32-34.
- [5] "The 6 Steps of the Wound Healing Process." *Advanced Tissue*. September 15, 2015. Accessed March 22, 2016.
- [6] Prakash, T. V., Ajay Chaudhary, Shyam Purushothaman, and Smitha KV. "Epidermal Grafting for Chronic Complex Wounds in India: A Case Series." *Cureus* 8, no. 3 (2016).
- [7] Shukla, V. K., Mumtaz A. Ansari, and S. K. Gupta. "Wound healing research: a perspective from India." *International Journal of Lower Extremity Wounds* 4, no. 1 (2005): 7-9.
- [8] Guo, S. al, and Luisa A. DiPietro. "Factors affecting wound healing." *Journal of dental research* 89, no. 3 (2010): 219-229.
- [9] Ding, Jie, Zengshuan Ma, Heather A. Shankowsky, Abelardo Medina, and Edward E. Tredget. "Deep dermal fibroblast profibrotic characteristics are enhanced by bone marrow-derived mesenchymal stem cells." *Wound Repair and Regeneration* 21, no. 3 (2013): 448-455.
- [10] Xu, Kedi, David Antonio Cantu, Yao Fu, Jaehyup Kim, Xiaoxiang Zheng, Peiman Hematti, and W. John Kao. "Thiol-ene Michael-type formation of gelatin/poly (ethylene glycol) biomatrices for three-dimensional mesenchymal

stromal/stem cell administration to cutaneous wounds. *Acta biomaterialia* 9, no. 11 (2013): 8802-8814.

- [11] Chen, Shixuan, Junbin Shi, Min Zhang, Yinghua Chen, Xueer Wang, Lei Zhang, Zhihui Tian et al. "Mesenchymal stem cell-laden anti-inflammatory hydrogel enhances diabetic wound healing." *Scientific reports* 5 (2015): 18104.
- [12] Otero-Viñas, Marta, and Vincent Falanga. "Mesenchymal stem cells in chronic wounds: the spectrum from basic to advanced therapy." *Advances in wound care* 5, no. 4 (2016): 149-163.
- [13] El Sadik, Abir O., Tarek A. El Ghamrawy, and Tarek I. Abd El-Galil. "The effect of mesenchymal stem cells and chitosan gel on full thickness skin wound healing in albino rats: histological, immunohistochemical and fluorescent study." *PloS one* 10, no. 9 (2015): e0137544.
- [14] An, Yulin, Huan Jing, Leiguo Ming, Shiyu Liu, and Yan Jin. "Bone marrow mesenchymal stem cell aggregate: an optimal cell therapy for full-layer cutaneous wound vascularization and regeneration." *Scientific reports* 5 (2015): 17036.
- [15] Ebaid, Hossam, Bahaa Abdel-Salam, Iftekhar Hassan, Jameel Al-Tamimi, Ali Metwalli, and Ibrahim Alhazza. "Camel milk peptide improves wound healing in diabetic rats by orchestrating the redox status and immune response." *Lipids in health and disease* 14, no. 1 (2015): 132.
- [16] Cereceres, Stacy, Tyler Touchet, Mary Beth Browning, Clayton Smith, Jose Rivera, Magnus Höök, Canaan Whitfield-Cargile, Brooke Russell, and Elizabeth Cosgriff-Hernandez. "Chronic wound dressings based on collagen-mimetic proteins." *Advances in wound care* 4, no. 8 (2015): 444-456.
- [17] Wang, Tao, Qisheng Gu, Jun Zhao, Jiakai Mei, Mingzhe Shao, Ye Pan, Jian Zhang, Haisheng Wu, Zhen Zhang, and Fang Liu. "Calcium alginate enhances wound healing by up-regulating the ratio of collagen types I/III in diabetic rats." *International journal of clinical and experimental pathology* 8, no. 6 (2015): 6636.

- [18] Aijaz, Ayesha, Renea Faulknor, François Berthiaume, and Ronke M. Olabisi. "Hydrogel microencapsulated insulin-secreting cells increase keratinocyte migration, epidermal thickness, collagen fiber density, and wound closure in a diabetic mouse model of wound healing." *Tissue Engineering Part A* 21, no. 21-22 (2015): 2723-2732.
- [19] Popov, S. V., and Yu S. Ovodov. "Polypotency of the immunomodulatory effect of pectins." *Biochemistry (Moscow)* 78, no. 7 (2013): 823-835.
- [20] Schmidgall, J., and A. Hensel. "Bioadhesive properties of polygalacturonides against colonic epithelial membranes." *International journal of biological macromolecules* 30, no. 5 (2002): 217-225.
- [21] Zheng, Long, Qi Hui, Lu Tang, Lulu Zheng, Zi Jin, Bingjie Yu, Zhitao Wang et al. "TAT-mediated acidic fibroblast growth factor delivery to the dermis improves wound healing of deep skin tissue in rat." *PloS one* 10, no. 8 (2015): e0135291.
- [22] Chan, Shu Wing Sophia. "Interleukin 2 Topical Cream for Treatment of Diabetic Foot Ulcer: Experiment Protocol." *JMIR research protocols* 4, no. 3 (2015).
- [23] Breuing, Karl, Christoph Andree, Giselle Helo, Jaromir Slama, Paul Y. Liu, and Elof Eriksson. "Growth factors in the repair of partial thickness porcine skin wounds." *Plastic and reconstructive surgery* 100, no. 3 (1997): 657-664.
- [24] Antoniadou, Harry N., Theofanis Galanopoulos, Janine Neville-Golden, Christopher P. Kiritsy, and Samuel E. Lynch. "Injury induces in vivo expression of platelet-derived growth factor (PDGF) and PDGF receptor mRNAs in skin epithelial cells and PDGF mRNA in connective tissue fibroblasts." *Proceedings of the National Academy of Sciences* 88, no. 2 (1991): 565-569.
- [25] Hans-Dietmar, B. E. E. R., Reinhard Fässler, and Sabine Werner. "Glucocorticoid-regulated gene expression during cutaneous wound repair." *Vitamins & hormones* 59 (2000): 217-239.

- [26] Harris, I. R., K. C. Yee, C. E. Walters, W. J. Cunliffe, J. N. Kearney, E. J. Wood, and E. Ingham. "Cytokine and protease levels in healing and non-healing chronic venous leg ulcers." *Experimental dermatology* 4, no. 6 (1995): 342-349.
- [27] Marikovsky, Moshe, Peter Vogt, Elof Eriksson, Jeffrey S. Rubin, William G. Taylor, Joachim Sasse, and Michael Klagsbrun. "Wound fluid-derived heparin-binding EGF-like growth factor (HB-EGF) is synergistic with insulin-like growth factor-I for Balb/MK keratinocyte proliferation." *Journal of investigative dermatology* 106, no. 4 (1996): 616-621.
- [28] Nishikawa, Kenichiro, Naohiro Seo, Mie Torii, Nei Ma, Daisuke Muraoka, Isao Tawara, Masahiro Masuya et al. "Interleukin-17 induces an atypical M2-like macrophage subpopulation that regulates intestinal inflammation." *PloS one* 9, no. 9 (2014): e108494.
- [29] McKay, I. A., and I. M. Leigh. "Epidermal cytokines and their roles in cutaneous wound healing." *British journal of dermatology* 124, no. 6 (1991): 513-518.
- [30] Gharaee-Kermani, Mehrnaz, and Sem H. Phan. "Role of cytokines and cytokine therapy in wound healing and fibrotic diseases." *Current pharmaceutical design* 7, no. 11 (2001): 1083-1103.
- [31] Grellner, W., T. Georg, and J. Wilske. "Quantitative analysis of proinflammatory cytokines (IL-1 $\beta$ , IL-6, TNF- $\alpha$ ) in human skin wounds." *Forensic science international* 113, no. 1 (2000): 251-264.
- [32] Feiken, Elles, John Rømer, Jens Eriksen, and Leif R. Lund. "Neutrophils express tumor necrosis factor- $\alpha$  during mouse skin wound healing." *Journal of investigative dermatology* 105, no. 1 (1995): 120-123.
- [33] Moore, Kevin W., Rene de Waal Malefyt, Robert L. Coffman, and Anne O'Garra. "Interleukin-10 and the interleukin-10 receptor." *Annual review of immunology* 19, no. 1 (2001): 683-765.
- [34] Mantovani, Alberto, Antonio Sica, Silvano Sozzani, Paola Allavena, Annunziata Vecchi, and Massimo Locati. "The chemokine system in diverse



- forms of macrophage activation and polarization." *Trends in immunology* 25, no. 12 (2004): 677-686.
- [35] Ferrante, Christopher J., and Samuel Joseph Leibovich. "Regulation of macrophage polarization and wound healing." *Advances in wound care* 1, no. 1 (2012): 10-16.
  - [36] Biswas, Subhra K., and Alberto Mantovani. "Macrophage plasticity and interaction with lymphocyte subsets: cancer as a paradigm." *Nature immunology* 11, no. 10 (2010): 889-896.
  - [37] Gordon, Siamon, and Fernando O. Martinez. "Alternative activation of macrophages: mechanism and functions." *Immunity* 32, no. 5 (2010): 593-604.
  - [38] Isidro, Raymond A., and Caroline B. Appleyard. "Colonic macrophage polarization in homeostasis, inflammation, and cancer." *American Journal of Physiology-Gastrointestinal and Liver Physiology* 311, no. 1 (2016): G59-G73.
  - [39] Dale, David C., Laurence Boxer, and W. Conrad Liles. "The phagocytes: neutrophils and monocytes." *Blood* 112, no. 4 (2008): 935-945.
  - [40] MacMicking, John, Qiao-wen Xie, and Carl Nathan. "Nitric oxide and macrophage function." *Annual review of immunology* 15, no. 1 (1997): 323-350.
  - [41] Wang, Yao-Chun, Fei He, Fan Feng, Xiao-Wei Liu, Guang-Ying Dong, Hong-Yan Qin, Xing-Bin Hu et al. "Notch signaling determines the M1 versus M2 polarization of macrophages in antitumor immune responses." *Cancer research* 70, no. 12 (2010): 4840-4849.
  - [42] Sridharan, Rukmani, Andrew R. Cameron, Daniel J. Kelly, Cathal J. Kearney, and Fergal J. O'Brien. "Biomaterial based modulation of macrophage polarization: a review and suggested design principles." *Materials Today* 18, no. 6 (2015): 313-325.
  - [43] Boehler, R. M., R. Kuo, S. Shin, A. G. Goodman, M. A. Pilecki, J. N. Leonard, and L. D. Shea. "Lentivirus delivery of IL-10 to promote and sustain

- macrophage polarization towards an anti-inflammatory phenotype." *Biotechnology and bioengineering* 111, no. 6 (2014): 1210-1221.
- [44] Spiller, Kara L., Sina Nassiri, Claire E. Witherel, Rachel R. Anfang, Johnathan Ng, Kenneth R. Nakazawa, Tony Yu, and Gordana Vunjak-Novakovic. "Sequential delivery of immunomodulatory cytokines to facilitate the M1-to-M2 transition of macrophages and enhance vascularization of bone scaffolds." *Biomaterials* 37 (2015): 194-207.
- [45] Jablonski, Kyle A., Stephanie A. Amici, Lindsay M. Webb, Juan de Dios Ruiz-Rosado, Phillip G. Popovich, Santiago Partida-Sanchez, and Mireia Guerau-de-Arellano. "Novel markers to delineate murine M1 and M2 macrophages." *PloS one* 10, no. 12 (2015): e0145342.
- [46] Acarregui, Argia, Ainhoa Murua, José L. Pedraz, Gorka Orive, and Rosa M. Hernández. "A perspective on bioactive cell microencapsulation." *BioDrugs* 26, no. 5 (2012): 283-301.
- [47] Uludag, Hasan, Paul De Vos, and Patrick A. Tresco. "Technology of mammalian cell encapsulation." *Advanced drug delivery reviews* 42, no. 1 (2000): 29-64.
- [48] Yu, Yang, Tingli Lu, Wen Zhao, Weiguang Sun, and Tao Chen. "Preparation and characterization of BSA-loaded microspheres based on polyanhydrides." *Journal of Applied Polymer Science* 121, no. 1 (2011): 352-358.
- [49] Coelho, M. J., A. Trigo Cabral, and M. H. Fernandes. "Human bone cell cultures in biocompatibility testing. Part I: osteoblastic differentiation of serially passaged human bone marrow cells cultured in  $\alpha$ -MEM and in DMEM." *Biomaterials* 21, no. 11 (2000): 1087-1094.
- [50] Mazzitelli, Stefania, Monica Borgatti, Giulia Breveglieri, Roberto Gambari, and Claudio Nastruzzi. "Encapsulation of eukaryotic cells in alginate microparticles: cell signaling by TNF-alpha through capsular structure of cystic fibrosis cells." *Journal of cell communication and signaling* 5, no. 2 (2011): 157-165.

- [51] Joki, Tatsuhiko, Marcelle Machluf, Anthony Atala, Jianhong Zhu, Nicholas T. Seyfried, Ian F. Dunn, Toshiaki Abe, Rona S. Carroll, and Peter McL Black. "Continuous release of endostatin from microencapsulated engineered cells for tumor therapy." *Nature biotechnology* 19, no. 1 (2001): 35-39.
- [52] Khattak, Sarwat F., Kyuon-sik Chin, Surita R. Bhatia, and Susan C. Roberts. "Enhancing oxygen tension and cellular function in alginate cell encapsulation devices through the use of perfluorocarbons." *Biotechnology and bioengineering* 96, no. 1 (2007): 156-166.
- [53] Muñoz, Marcelo, Ricardo Cedeño, Jenny Rodríguez, Wil PW van der Knaap, Eric Mialhe, and Evelyne Bachère. "Measurement of reactive oxygen intermediate production in haemocytes of the penaeid shrimp, *Penaeus vannamei*." *Aquaculture* 191, no. 1 (2000): 89-107.
- [54] McWhorter, Frances Y., Tingting Wang, Phoebe Nguyen, Thanh Chung, and Wendy F. Liu. "Modulation of macrophage phenotype by cell shape." *Proceedings of the National Academy of Sciences* 110, no. 43 (2013): 17253-17258.